© 2015. Published by The Company of Biologists Ltd | Development (2015) 142, 3033-3045 doi:10.1242/dev.120824

RESEARCH ARTICLE

Protein phosphatase 2A promotes the transition to G0 during terminal differentiation in *Drosophila*

Dan Sun and Laura Buttitta*

ABSTRACT

Protein phosphatase type 2A complex (PP2A) has been known as a tumor suppressor for over two decades, but it remains unclear exactly how it suppresses tumor growth. Here, we provide data indicating a novel role for PP2A in promoting the transition to quiescence upon terminal differentiation *in vivo*. Using *Drosophila* eyes and wings as a model, we find that compromising PP2A activity during the final cell cycle prior to a developmentally controlled cell cycle exit leads to extra cell divisions and delays entry into quiescence. By systematically testing the regulatory subunits of *Drosophila* PP2A, we find that the B56 family member *widerborst* (*wdb*) is required for the role of PP2A in promoting the transition to quiescence. Cells in differentiating tissues with compromised PP2A retain high Cdk2 activity when they should be quiescent, and genetic epistasis tests demonstrate that ectopic Cyclin E/Cdk2 activity is responsible for the extra cell cycles caused by PP2A inhibition. The loss of *wdb*/PP2A function cooperates with aberrantly high Cyclin E protein levels, allowing cells to bypass a robust G0 late in development. This provides an example of how loss of PP2A can cooperate with oncogenic mutations in cancer. We propose that the PP2A complex plays a novel role in differentiating tissues to promote developmentally controlled quiescence through the regulation of Cyclin E/Cdk2 activity.

KEY WORDS: Cell cycle, Quiescence, Terminal differentiation

INTRODUCTION

In adult metazoans, most terminally differentiated cells exit from the cell cycle and lie in a state of prolonged or permanent quiescence. The transition from active proliferation to quiescence *in vivo* is robust, often irreversible, and ensured by redundant cell cycle regulatory mechanisms (Buttitta et al., 2007; Firth and Baker, 2005; Nicolay et al., 2010; Pajcini et al., 2010; Wirt et al., 2010). By comparison, most studies of quiescence have been performed in cell culture, where contact inhibition, drug treatments or withdrawal of mitogens induce a quiescent state that is most often readily reversible (Coller, 2011). Although some of the key cell cycle regulators promoting quiescence in these contexts overlap [e.g. Retinoblastoma (RB) family members, Cyclin-dependent kinase inhibitors (CKIs)], there must be key differences between the reversible quiescence in cell culture and developmentally controlled robust cell cycle exit *in vivo*.

Recent work in mammalian cell culture has demonstrated that the level of Cdk2 activity after mitosis impacts the proliferation versus quiescence decision for the next cell cycle, such that cells with low Cdk2 activity enter a quiescent 'G0-like' state (Spencer et al., 2013). This suggests that mechanisms regulating Cyclin/Cdk2 activity during the final cell cycle *in vivo* could impact the timing and robustness of cell cycle exit in tissues. Consistent with this hypothesis, the loss of CKIs that inhibit Cyclin E/Cdk2 complexes or loss of the F-box protein Fbw7 (Fbxw7), which regulates Cyclin E stability, can partially delay proper cell cycle exit in certain tissues (Chen and Segil, 1999; de Nooij et al., 1996; Fero et al., 1996; Kiyokawa et al., 1996; Lane et al., 1996; Minella et al., 2008; Moberg et al., 2001; Tane et al., 2014). But even in the presence of aberrantly high Cyclin E/Cdk2, cell cycle exit is most often only delayed by one or two cell cycles *in vivo*, demonstrating the robustness of developmentally controlled quiescence (Baumgardt et al., 2014; Buttitta et al., 2010; Loeb et al., 2005; Nakayama et al., 1996).

Determining which cell cycle regulators are required for developmentally controlled cell cycle exit *in vivo* has posed some challenges. Redundancy in the function of multiple paralogs for each cell cycle regulator makes genetic analysis complicated, with studies often encompassing double or triple mutants (Gui et al., 2007; Wirt et al., 2010; Zindy et al., 1999). In addition, the late stage of development at which cell cycle exit occurs and the asynchronous nature of cell cycle exit in many tissues requires conditional genetic manipulations and timecourse analysis of samples. *Drosophila* eyes and wings have provided an advantageous system with which to study this process, as they undergo a relatively synchronized cell cycle exit during metamorphosis, have fewer paralogs and there are tools for precise conditional genetic manipulations. We used this system to examine cell cycle exit in terminally differentiating tissues and found that even in RB family member Rbf1 (Rbf – FlyBase)-deficient cells, Cyclin E/Cdk2 overexpression delays but cannot bypass cell cycle exit (Buttitta et al., 2007), suggesting that additional downstream mechanisms ensure the transition from proliferation to quiescence *in vivo* (Ehmer et al., 2014; Nicolay et al., 2010; Simon et al., 2009).

To identify additional mechanisms ensuring cell cycle exit, we examined *Drosophila* homologs of several tumor suppressor proteins expected to play a role in promoting quiescence. PP2A has been recognized as a tumor suppressor for over two decades (Janssens et al., 2005), but the molecular mechanism for PP2A in tumor suppression remains unknown. PP2A dephosphorylates RB family members to inhibit cycling (Kolupaeva and Janssens, 2013; Kurimchak and Grana, 2013), and removes an essential activating phosphorylation on the Cdk2 T-loop *in vitro* (Poon and Hunter, 1995). We therefore examined whether PP2A plays multiple, redundant roles to promote the developmentally controlled robust cell cycle exit *in vivo*.

Here, we show that cells with reduced PP2A function fail to transition to a quiescent state at the normal developmental time. Loss of PP2A function specifically during the final cell cycle leads ~10% of cells to perform an extra cycle before entry into permanent quiescence. Cells with compromised PP2A exhibit increased Cdk2

University of Michigan, Department of Molecular, Cellular and Developmental Biology, Ann Arbor, MI 48109, USA.

*Author for correspondence (buttitta@umich.edu)

Received 8 December 2014; Accepted 28 July 2015

Development (2015) 142, 3033-3045 doi:10.1242/dev.120824

activity and aberrant E2F transcriptional activity. In the presence of high, oncogenic Cyclin E levels the loss of PP2A function allows cells to bypass a robust G0 mechanism during late stages in fly development. The PP2A enzyme is directed to distinct substrates via associations with different regulatory subunits, which can be highly dynamic during development. We show that the PP2A B56 regulatory subunit *widerborst* (*wdb*) is specifically required for the PP2A-mediated transition between proliferation and quiescence. Furthermore, this new function for PP2A/Wdb occurs even in the complete absence of RB/E2F/DP function, suggesting that it acts through downstream targets directly on the cell cycle machinery to promote quiescence *in vivo*.

RESULTS

Loss of PP2A delays the transition to quiescence *in vivo*

We performed a small-scale RNAi-based screen of ~500 randomly chosen Harvard Transgenic RNAi Project (TRiP) lines to identify new potential tumor suppressor genes involved in the proper timing of the developmentally controlled quiescence in the *Drosophila* eye. The primary screen was an adult eye color-based screen, an adaptation of the method described by Bandura et al. (2013). This was followed by a secondary, dissection-based screen to determine which hits from the initial screen effectively compromised cell cycle exit. Normally, the *Drosophila* eye becomes completely quiescent by 24 h after pupa formation (APF) (Buttitta et al., 2007). We therefore looked for RNAis that compromised quiescence, leading to ectopic cell cycles at 24 h APF. We used the *Glass Multimer Reporter* (*GMR*)-*Gal4* (Ellis et al., 1993) driver to express UAS-controlled RNAi lines, and assayed for ectopic S phases by EdU incorporation (Buck et al., 2008) and ectopic expression of a cell cycle transcriptional reporter *PCNA-GFP* (Thacker et al., 2003) in eyes after normal quiescence from 24-30 h APF (supplementary material Fig. S1). Importantly, the *GMR-Gal4* driver activates the UAS-RNAi specifically during the final cell cycle in the eye, thereby avoiding earlier deleterious effects. We found that two independent RNAi lines to the *Drosophila* PP2A catalytic subunit *microtubule star* (*mts*) and one to the sole PP2A scaffold A subunit *Pp2A-29B* caused ectopic S phases and cell cycle gene expression, at time points when the *Drosophila* eye should be fully quiescent (supplementary material Fig. S1A-C).

To confirm the RNAi results, we overexpressed a dominant-negative form of *mts* (mts^{DN}) during the final cell cycle in fly eyes and found that it fully recapitulated the RNAi phenotypes. mts^{DN} is a truncation that interacts non-productively with PP2A scaffolding (A) and regulatory (B) subunits, and serves as an effective competitive inhibitor when overexpressed (Evans et al., 1999). To test whether the role of PP2A in quiescence is eye specific, we overexpressed mts^{DN} in the posterior wing during the final one to two cell cycles using *engrailed-Gal4*, modified with a temperature-sensitive *Gal80*^{TS} (en^{TS}; see Materials and Methods for details). Similar to the eye, we observed ectopic S phases by EdU incorporation and ectopic mitoses by staining for phosphorylation of serine 10 on Histone H3 (PH3) at 24-28 h APF, time points when few cell cycles are normally observed in the wing (Fig. 1A,B). Overexpression of a functional wild-type *mts* (mts^{WT}) had no observable effect on quiescence in these tissues (Fig. 1C,D), confirming that the observed phenotype is due to the loss of PP2A function.

We performed a timecourse and quantification of the mitoses in wings expressing mts^{DN} (Fig. 1E; supplementary material Fig. S1D) or PP2A RNAi (Fig. 1F), which revealed continued mitoses in eyes and wings until 37 h APF, 13 h after the normal cell cycle exit in these tissues (Buttitta et al., 2007; Milan et al., 1996; Schubiger and Palka, 1987). To confirm the staining results, we measured the DNA content of pupal eyes expressing mts^{DN} by flow cytometry. As expected from the ectopic cell cycle markers, an increased proportion of cells containing greater than 2C DNA content

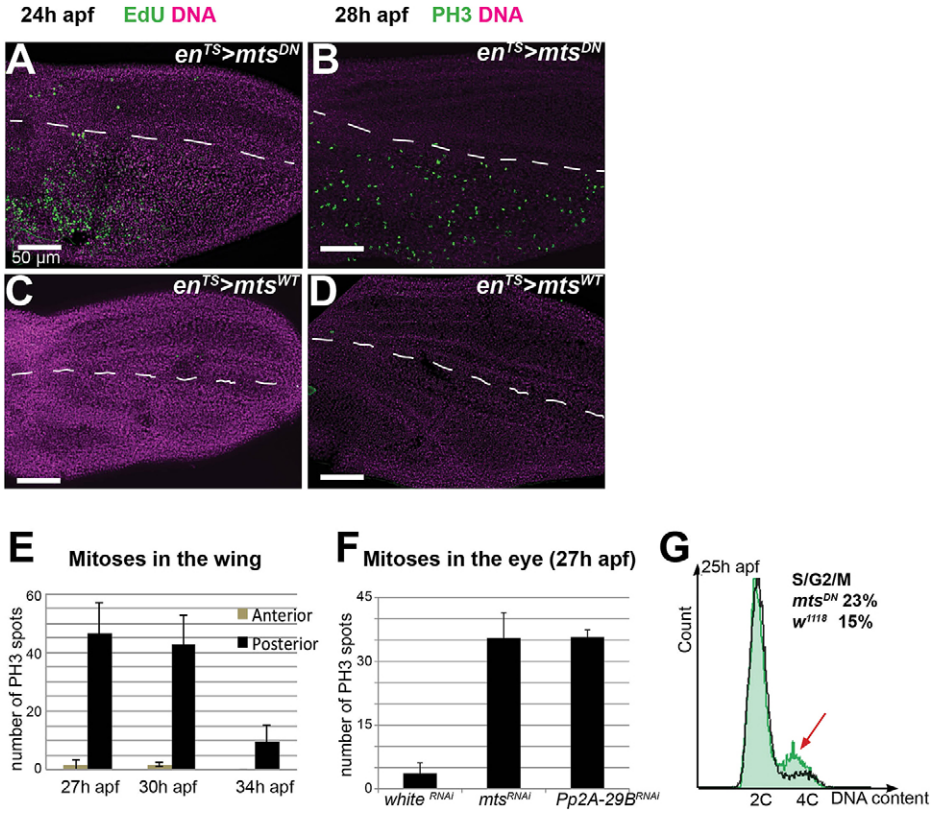

Fig. 1. PP2A promotes the timely transition to quiescence *in vivo*. (A-D) Expression of a dominant-negative *mts* (mts^{DN}, A,B) or wild-type *mts* (mts^{WT}, C,D) was restricted to the posterior wing during late larval stages using the *engrailed-Gal4*/*Gal80*^{TS},*UAS* system (en^{TS}). Pupal tissues were dissected at 24 h APF and labeled with EdU for 1 h to visualize S phase (A,C) or labeled with anti-PH3 to visualize mitoses at 28 h APF (B,D). In regions where PP2A function is compromised by mts^{DN}, cells continue cycling when they should be postmitotic. The dashed line indicates the anterior-posterior boundary. (E,F) Quantification of ectopic mitoses in pupal tissues at different time points during normally postmitotic stages reveals a delay of cell cycle exit by ~10 h in mts^{DN} or PP2A RNAi. Error bars indicate s.e.m. (G) Flow cytometry was used to assess the DNA content of 25 h APF eyes with mts^{DN} expression (green trace) or controls (black trace). The arrow indicates an increase in cells with non-G1 DNA content.

Development (2015) 142, 3033-3045 doi:10.1242/dev.120824

was observed in mts^{DN}-expressing eyes as compared with stage-matched controls without transgene expression (Fig. 1G). However, after 37 h APF, eyes expressing mts^{DN} exit the cell cycle with a normal G1 DNA content. Altogether, our data suggest that inhibition of PP2A during the final cell cycle causes a temporary delay of the transition to quiescence in a compartment-autonomous manner.

Inhibition of PP2A leads to an extra cell cycle during the delay of quiescence

We next investigated whether the delayed transition to quiescence caused by loss of PP2A leads to additional cell cycles or whether it is the result of a prolonged final cell cycle. We performed a clonal analysis to count the number of cells per clone, which reflects the number of cell divisions before quiescence, using the *heat shock* (*hs*)-*flp actin>stop>Gal4/UAS* 'flip-out' system. In brief, with this system a precisely timed heat shock leads to random cis-recombination between FRT sites (indicated by >) flanking a stop codon. Cells in which recombination occurs flip-out the stop codon to allow Gal4-mediated gene expression, which continues permanently in all daughter cells (Pignoni and Zipursky, 1997). In this manner, the number of daughter cells can be counted after the delayed quiescence at 37 h APF. Non-overlapping clones were induced at 0 h APF (just prior to the final cycle) by a short heat shock at 37°C. Transgenes to manipulate PP2A activity, as well as GFP to mark clones, and an apoptosis inhibitor (P35; to prevent loss of daughters, which confounds clonal cell counts) were expressed and cells per clone were counted blind for at least 100 clones in the wing blade at 42-44 h APF (Fig. 2A; supplementary material Fig. S1G). Most (95%) control clones expressing GFP and P35 contain two cells or fewer per clone, as the induction of the recombination occurs during or just prior to the final cycle. However, 15% of clones expressing mts^{DN} contain more than two cells per clone, which indicates that ~10% of mts^{DN}-expressing cells undergo an extra cell cycle before entering G0. For comparison, when the G1 cyclin complex Cyclin D/Cdk4 is directly overexpressed via *Gal4/UAS*, we observe 50% of cells performing an extra cell cycle, before becoming quiescent at 36 h APF (Buttitta et al., 2007).

To determine whether PP2A inhibition also causes extra cell cycles in the eye, we examined the morphology of the fly eye at late

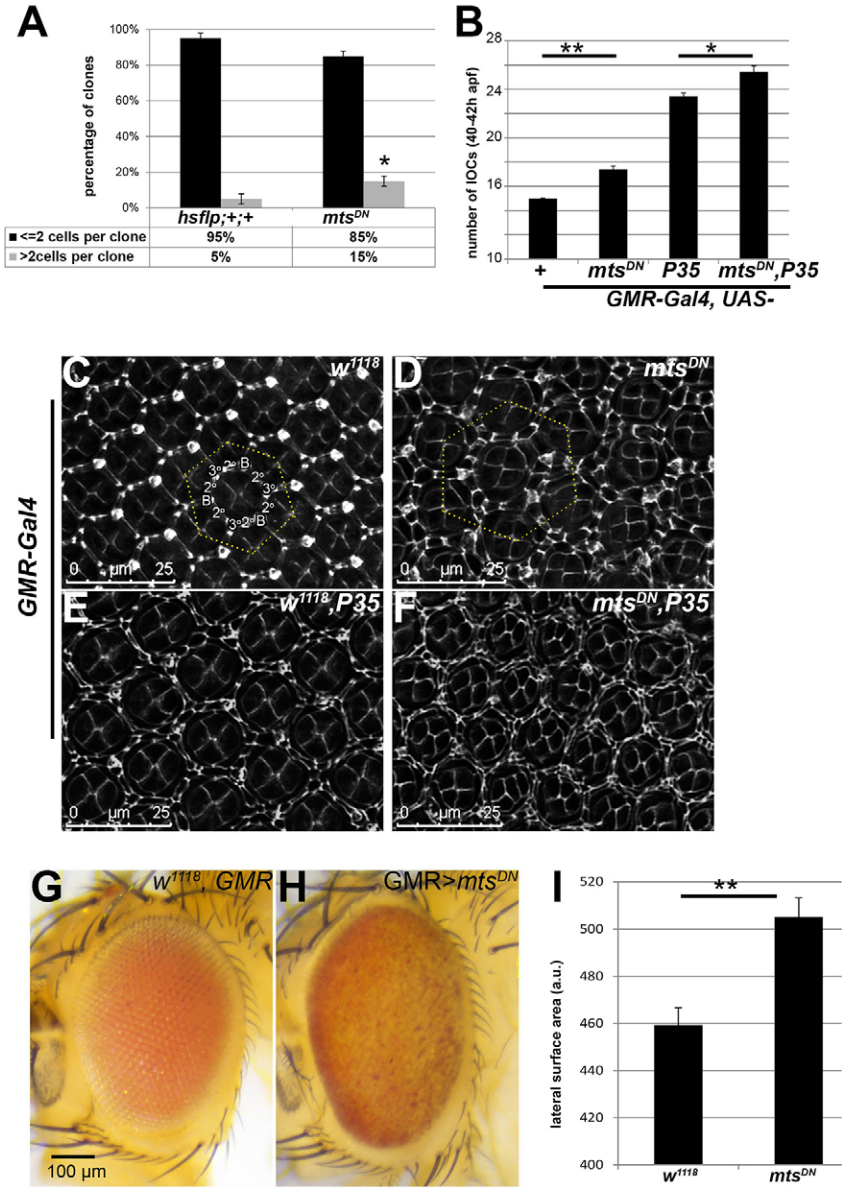

Fig. 2. PP2A inhibition during the final cell cycle leads to extra cell divisions during tissue development. (A) Clonal lineage analysis in the wing was used to measure the number of cell cycles before entry into quiescence. GFP-marked clones were induced at the start of metamorphosis (0 h APF) during the final cell cycle using the *hs-flp actin>Gal4/UAS* system. Wings were examined 42-44 h later and cells/clones were quantified for at least 100 clones/genotype. Clones also express the apoptosis inhibitor P35. Approximately 10% of cells undergo an extra cell cycle when PP2A is inhibited during the final cell cycle to generate an increase in clones with more than 2 cells. (B-F) *GMR-Gal4/UAS* was used to drive expression of the indicated transgenes in the eye, specifically during the final cell cycle. Quantification of interommatidial cell (IOC) number was performed at 40-42 h APF in retinas stained for Discs large (Dlg) to reveal cell morphology. Cell types of IOCs are labeled as: B, bristles; 2°, secondary pigment cell; 3°, tertiary pigment cell. IOCs are shared by adjacent ommatidia and the number of IOCs was quantified within an ommatidial group (OG) that covers a defined hexagonal area (bordered by yellow dots in C,D). The secondary pigment cells crossed by the hexagonal boundary were counted as half. At least 15 OGs were scored from independent samples for each genotype (B). Representative examples are shown for w^{1118} (C), *GMR*>mts^{DN} (D), *GMR*>P35 (E) and *GMR*>P35 +mts^{DN} (F). (G-I) The lateral surface area of adult fly eyes was measured and compared between w^{1118}, *GMR* (G) and *GMR*>mts^{DN} (H). n=8 for I. Error bars indicate s.e.m. *P<0.05, **P<0.01 (Student's t-test).

Development (2015) 142, 3033-3045 doi:10.1242/dev.120824

pupal stages (40-42 h APF). In wild-type or control retinas (Fig. 2B), the apical ommatidial structure consists of four cone cells in the center surrounded by interommatidial cells (IOCs) (Tomlinson and Ready, 1987). The IOCs are shared by adjacent ommatidial cores and the number of IOCs can be quantified within an ommatidial group (OG) that covers a defined hexagonal area (Fig. 2D) (Ou et al., 2007). When PP2A is inhibited during the final cell cycle in the eye, extra IOCs are observed (17.4±0.3 cells/OG), consistent with approximately one extra cell cycle per OG. We confirmed that the extra cycles are not due to disruption of programmed cell death in the pupal eye, as the cell number is further increased when apoptosis is inhibited (Fig. 2E,F). The size of the adult eye is also increased when PP2A is inhibited (Fig. 2H). Our cell count data suggest that PP2A inhibition enlarges the eye partly by ectopic cell proliferation, but we also consistently observed an increase in cell size. An increase in cell size is consistent with known functions of PP2A in the TOR/S6 kinase (S6K) pathway (Bielinski and Mumby, 2007; Hahn et al., 2010).

PP2A counteracts the phosphorylation of S6K, which we used as an assay to confirm the activity of our *mts* transgenes (supplementary material Fig. S2A). To test whether the increase in active phospho-S6K impacts the transition to quiescence, we overexpressed the GTPase *Rheb*, which increases cellular growth, TOR signaling and phospho-S6K (Saucedo et al., 2003). We did not observe any delay in cell cycle exit in the pupal wing, nor extra IOCs in the retina when *Rheb* was overexpressed, despite increased phospho-S6K (supplementary material Fig. S2). We therefore suggest that the function of PP2A in the transition to quiescence is independent of its role in regulating phospho-S6K.

Inhibition of PP2A leads to ectopic Cdk2 activity

Proper cell cycle exit in *Drosophila* eyes and wings is ensured by inhibition of E2F/DP-mediated transcription and suppression of Cyclin E (CycE)/Cdk2 activity (Buttitta et al., 2007; Firth and Baker, 2005). To examine whether cells with inhibited PP2A retain high Cdk2 activity, we used MPM2 antibody staining as an *in vivo* readout for ectopic Cdk2 activity at time points after normal cell cycle exit. MPM2 antibodies detect nuclear Cdk2 phospho-epitopes on the histone locus body (HLB) that normally occur only during S phase in proliferating cells, in addition to the well-described cytoplasmic epitopes present during mitosis (White et al., 2011, 2007). We generated GFP-marked clones in eyes and wings expressing CycE/Cdk2 as a positive control, mts^{DN} or mts^{WT} during the final one to two cell cycles and examined MPM2 reactivity at 26 h APF, 2 h after normal cell cycle exit. We observed abundant nuclear HLB staining by MPM2 in cells expressing *CycE/Cdk2* and mts^{DN}, but no MPM2 staining in cells expressing mts^{WT} (Fig. 3A-C). This suggests that loss of PP2A leads to ectopic Cdk2 activity in normally postmitotic tissues.

We next tested whether loss of PP2A also leads to a failure to repress E2F/DP transcriptional activity during normal cell cycle exit. We used the E2F-responsive *Proliferating cell nuclear antigen* (*PCNA*) promoter fused to *GFP* (Thacker et al., 2003) as a readout of ectopic E2F activity at time points after normal cell cycle exit. Compromising PP2A function in eyes during the final cell cycle led to ectopic E2F activity at 26 h APF, a time point when little to no E2F activity should persist (Fig. 3D,E).

The repression of E2F/DP-mediated transcription upon cell cycle exit is modulated by RB binding, which is inhibited by RB phosphorylation via active Cyclin/Cdk complexes or promoted by dephosphorylation via phosphatases. In mammals, PP2A can modulate the phosphorylation state of the RB-related pocket protein p107 (Rbl1) to promote cell cycle exit in chondrocytes (Jayadeva et al., 2010; Kolupaeva et al., 2008; Kurimchak et al., 2013). Thus, a plausible mechanism for PP2A regulation of the transition to quiescence could be through inhibition of *Drosophila* retinoblastoma family (Rbf)-mediated repression of E2F/DP transcriptional activity. To genetically test whether endogenous E2F/DP complexes are required for the delay of quiescence caused by PP2A loss, we used the MARCM system (Lee and Luo, 2001) to create *Dp* homozygous null mutant clones (supplementary material Fig. S3), with and without PP2A inhibition. *Dp* null mutant cells exhibit defects in cell proliferation and *Dp* null mutant clones in larval wings are on average 30.6% the size of wild-type clones generated in parallel (Nicolay and Frolov, 2008). We confirmed a similar phenotype for *Dp* mutant clones in pupal wings, which are 32.7% the size of wild-type clones induced in parallel (Fig. 3G; supplementary material Fig. S3), and we verified that *Dp* mutant clones of this size in the pupal wing lack Dp protein (Fig. 3H,I). *Dp* null mutant clones expressing mts^{DN} in pupal wings exhibit ectopic mitoses in wings at time points after normal cell cycle exit, whereas no mitoses were observed in any stage-matched *Dp* null mutant clones (Fig. 3G,H). This suggests that the delay of cell cycle exit upon inhibition of PP2A is epistatic to E2F/DP function, and reveals an additional role for PP2A in promoting quiescence that is independent of RB/E2F/DP complexes *in vivo*.

Inhibition of PP2A function does not delay cell cycle exit by preventing APC/C activity

The Anaphase-promoting complex/Cyclosome (APC/C) promotes timely cell cycle exit in *Drosophila* eyes and wings by degrading residual Cyclin A (CycA) and Cyclin B (CycB) during the final G1 (Buttitta et al., 2010; Ruggiero et al., 2012; Tanaka-Matakatsu et al., 2007). Furthermore, the APC/C complex can cooperate with RB proteins to reinforce cell cycle exit by promoting degradation of Skp2, which targets CKIs for destruction (Binné et al., 2007). PP2A can impact APC/C indirectly by counteracting CycB/Cdk1 phosphorylations (Hunt, 2013), as well as regulating the binding and stability of the APC/C inhibitor Emi (Wu et al., 2007), which functions similarly to *Drosophila Regulator of cyclin A1* (*Rca1*) (Grosskortenhaus and Sprenger, 2002). We therefore examined whether APC/C function is inhibited when PP2A is compromised, leading to a delay in cell cycle exit. As a read-out for APC/C activity, we examined the levels of the known APC/C target CycB by immunohistochemistry. GFP-marked clones with transgene expression were induced by the flip-out Gal4/UAS/$Gal80^{TS}$ system and shifted to permissive temperature during late larval stages (Fig. 4A-C). As a positive control, we inhibited APC/C activity by expression of *Rca1* and observed clear CycB accumulation in GFP-positive cells in the posterior of larval eye imaginal discs (Fig. 4A,A′). However, we observed no change in CycB levels in eyes with either PP2A loss-of-function via mts^{DN} expression or PP2A gain-of-function with mts^{WT} (Fig. 4B-C′). We also extracted protein samples from late larval eye imaginal discs and performed western blots to measure total levels of CycA and CycB. We found that neither gain-of-function nor loss-of-function of PP2A significantly increased CycA or CycB levels (Fig. 4D,E).

We next examined whether CycB/Cdk1 complex activation is altered by PP2A inhibition during cell cycle exit *in vivo*. The activation of the CycB/Cdk1 complex is triggered by the removal of inhibitory phosphates on Cdk1 (at Y14 and T15) by the phosphatase Cdc25c, termed String in *Drosophila*. The activity of String is rate limiting for entry into mitosis in the wings and eyes *in vivo* (Neufeld et al., 1998) and persistent CycB/Cdk1 activity could delay proper

Development (2015) 142, 3033-3045 doi:10.1242/dev.120824

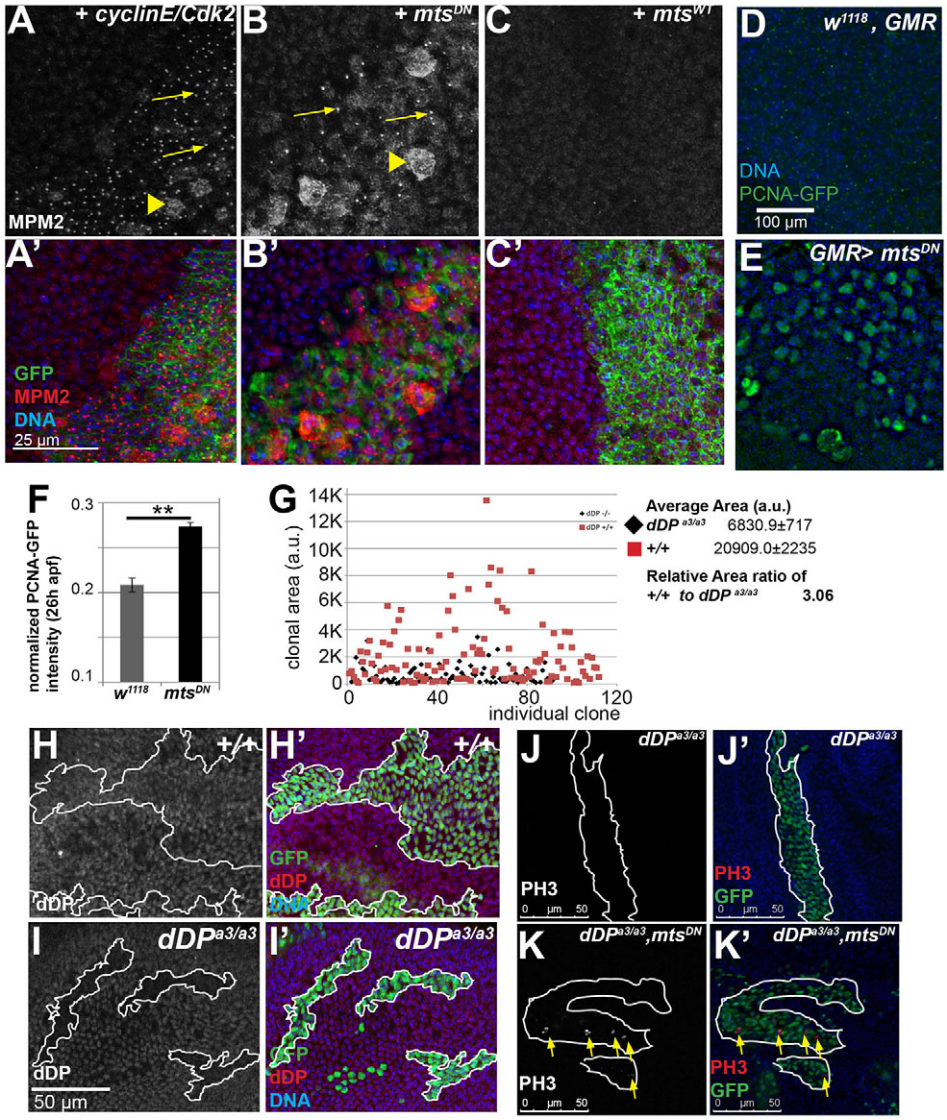

Fig. 3. Inhibition of PP2A leads to ectopic Cdk2 and E2F activity during the final cell cycle. (A-C′) Pupal wings containing clones expressing the indicated transgenes at 24 h APF via the *hs-flp actin>Gal4/UAS* system were stained with MPM2 antibody. MPM2 recognizes subnuclear foci (arrows) corresponding to Cdk2 phosphorylated epitope(s) at the histone locus body. This is in contrast to the cytoplasmic staining (arrowhead) that indicates mitotic MPM2 phospho-epitopes. (A,A′) *CycE/Cdk2* overexpression results in MPM2 foci within clones. (B,B′) Inhibition of PP2A function via expression of mts^{DN} leads to MPM2 subnuclear foci. (C,C′) No ectopic MPM2 foci are observed in clones expressing mts^{WT}. (D,E) Pupal eyes were assessed at 26 h APF, a stage that is normally postmitotic, for E2F transcriptional activity using the *PCNA-GFP* reporter transgene. (E) Expression of mts^{DN} during the final cell cycle via *GMR-Gal4/UAS* leads to ectopic E2F activity when tissues should be postmitotic. (F) Quantification of PCNA-GFP reporter intensity was normalized to DNA content and compared between control (w^{1118}) and mts^{DN}. Error bars indicate s.e.m. $^{**}P<0.01$ (Student's *t*-test). (G-K′) Wild-type or Dp^{a3} null mutant clones were induced using the MARCM system by a 20 min heat shock at 37°C at early L3 stage. Clones were examined and measured at 24-26 h APF. (G) A scatter plot of clone sizes reveals that the average area of Dp^{a3} null mutant clones compared with wild-type control MARCM clones generated in parallel. (H-I′) Wild-type or Dp^{a3} null mutant clones were stained with Dp antibody. Dp^{a3} mutant clones lack Dp protein. (J-K′) Loss of PP2A delays cell cycle exit independently of E2F activity. *Dp* null mutant clones (J,J′) or *Dp* null mutant clones expressing mts^{DN} (K,K′) were induced as above, and assayed for ectopic mitoses via anti-PH3 at a time that is normally postmitotic (26 h APF). Clones were marked by GFP. White lines outline the clones and yellow arrows indicate ectopic mitoses within the clones.

cell cycle exit. However, we did not observe significant effects on Cdk1 inhibitory phosphorylations upon genetic manipulations of PP2A activity (Fig. 4F), in contrast to the ectopic expression of *string*, which strongly reduces Cdk1 inhibitory phosphorylation, as expected (Fig. 4F).

PP2A interacts with negative regulators of CycE/Cdk2 activity *in vivo*

Consistent with the evidence of ectopic Cdk2 activity when PP2A is compromised (Fig. 3A-C), we also observed functional genetic interactions between known negative regulators of Cdk2 activity and PP2A in the fly eye (Fig. 5). The sole p21/p27 (Cdkn1a/b) CKI in *Drosophila*, *dacapo* (*dap*), is a major inhibitor of the CycE/Cdk2 complex upon cell cycle exit (de Nooij et al., 1996; Lane et al., 1996; Sukhanova and Du, 2008). We examined whether loss of *dap* cooperates with inhibition of PP2A to delay quiescence by quantifying IOCs in late pupal stages as described previously for Fig. 2. The loss of one copy of *dap* (using the dap^4 null allele) enhanced the effect of mts^{DN} expression (driven by *GMR-Gal4*) on the number of IOCs (18.7±0.3), compared with PP2A inhibition alone (17.3±0.2) (Fig. 5A-D). We also observed a 15% increase in adult eye size in *dap* heterozygotes expressing mts^{DN} compared with

Development (2015) 142, 3033-3045 doi:10.1242/dev.120824

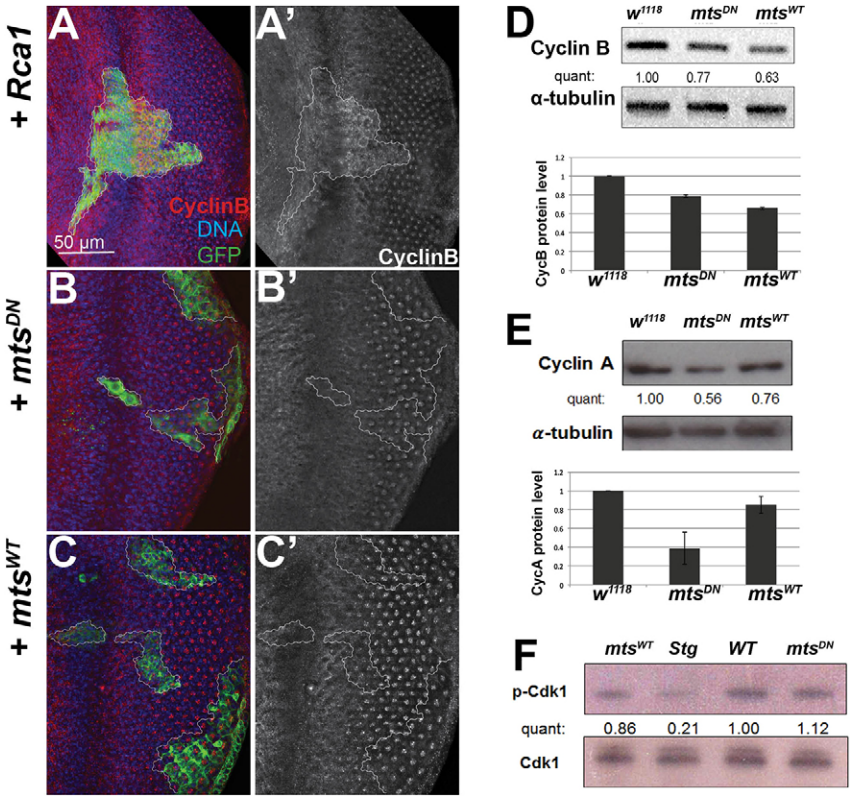

Fig. 4. APC/C activity is not compromised by reduced PP2A function during the final cell cycle. (A-C′) Late L3 instar larval eye imaginal discs were isolated and stained with anti-CycB. Clones were induced by the *hs-flp actin>Gal4/UAS* system and marked by GFP. As a positive control, overexpression of *Rca1* (A,A′) resulted in accumulation of CycB protein via inhibition of APC/C. By contrast, no obvious change in CycB level was observed for either mts^{DN} (B,B′) or mts^{WT} (C,C′) overexpression. Note that CycB staining is observed in R8 photoreceptors as previously described (Ruggeiro et al., 2012). Clones are outlined. (D-F) Western blots of CycB, CycA or phospho-Cdk1 (p-Cdk1) levels with mts^{DN} or mts^{WT} overexpression. Protein samples were collected from either late L3 instar larval eye imaginal discs with transgene expression under control of *GMR-Gal4* (D,E) or late L3 instar larval heads with transgene expression induced by the *hs-flp actin>Gal4/UAS* system (F). Altering PP2A activity did not increase CycB or CycA, nor strongly alter the ratio of p-Cdk1/total Cdk1. Note that expression of the Cdk1 phosphatase String (Stg) significantly reduces p-Cdk1, and serves as a positive control. Bar charts show the quantification of signal intensities from two independent experiments. Error bars indicate s.e.m.

siblings with normal *dap*, while mts^{DN} expression alone caused a ~8% increase in adult eye size (Fig. 5E). In addition, we used the MARCM system to create *dap* homozygous null mutant clones, with and without PP2A inhibition via expression of mts^{DN}. In *dap* null mutant clones expressing mts^{DN} we also observed an increase in extra cells, including an increase in lens-producing cone cells, which is rarely seen in wild-type clones expressing mts^{DN} (Fig. 5G-I; supplementary material Fig. S4I). In a reciprocal experiment, we overexpressed *dap* together with mts^{DN} during the final cell cycle using the *GMR-Gal4* driver, and observed a partial suppression of the enlarged eye phenotype caused by PP2A inhibition alone (Fig. 5F). This indicates that high Cdk2 activity is, at least in part, required for the enlarged eye phenotype resulting from PP2A inhibition.

To confirm that the enhancement of the *dap* eye phenotypes by mts^{DN} was due to impacts on CycE/Cdk2 function, we next examined a different negative regulator of CycE for genetic interactions with PP2A. The CycE protein level is controlled by the SCF complex with the ubiquitin ligase Fbw7, termed Archipelago (Ago) in *Drosophila*. Loss of *ago* in the fly leads to aberrant accumulation of CycE protein and temporarily delays cell cycle exit of the bristle precursors in the eye (Moberg et al., 2001). Consistent with our results from loss of one copy of *dap*, we found that loss of one copy of *ago* (using the ago^1 allele) also enhanced the mts^{DN} large eye phenotype (supplementary material Fig. S4).

We next examined whether modulation of PP2A activity itself could impact CycE protein levels or stability during the final cell cycle. We used *GMR-Gal4* to drive expression of mts^{DN} or mts^{WT} during the final cell cycle in the eye and extracted protein from larval eyes for western blot analysis. We observed no significant increase in CycE protein levels when PP2A was compromised (supplementary material Fig. S4). Altogether, our genetic data indicate that PP2A acts through a pathway that is independent of RB/E2F/DP, and possibly in parallel to *dap* or *ago* to regulate CycE/Cdk2 activity.

PP2A inhibition cooperates with high CycE levels to bypass robust cell cycle exit

High CycE/Cdk2 activity during the final cell cycle in fly tissues delays cell cycle exit, but after only a few extra cell cycles a robust cell cycle exit mechanism ensures permanent quiescence (Baumgardt et al., 2014; Buttitta et al., 2010, 2007). We asked whether PP2A inhibition could promote cells with aberrantly high CycE expression to override the robust transition to quiescence and maintain proliferation during later stages of development, as suggested by its known role as a tumor suppressor. We used *GMR-Gal4* to drive *UAS-CycE* expression together with the baculoviral apoptosis inhibitor P35 (to minimize corrective apoptosis) with or without PP2A inhibition via mts^{DN}. We examined proliferation in the eye at late pupal stages, several hours after the normal robust exit that occurs even in the presence of dysregulated CycE (Fig. 6A-D).

Pupal eyes expressing CycE without any PP2A modulation exhibit few S phases and mitoses at this late stage of development, whereas eyes expressing CycE together with mts^{DN} maintain high proliferation even after the stage normally associated with robust, permanent cell cycle exit. To confirm this, we isolated late pupal eyes and performed flow cytometry to examine their DNA content at 46 h APF. When eyes overexpress CycE, only ~9% of cells from the entire retina exhibit an abnormal S/G2 DNA content. By contrast, when PP2A is compromised in stage-matched eyes overexpressing CycE, 27% of cells exhibit abnormal S/G2 DNA contents (Fig. 6F). This suggests that PP2A normally functions as a barrier to limit the bypass of cell cycle exit when CycE is dysregulated *in vivo*.

The PP2A B56 subunit Widerborst regulates the transition to quiescence *in vivo*

To identify the PP2A regulatory subunit responsible for promoting quiescence in differentiating tissues, we systematically tested each

Development (2015) 142, 3033-3045 doi:10.1242/dev.120824

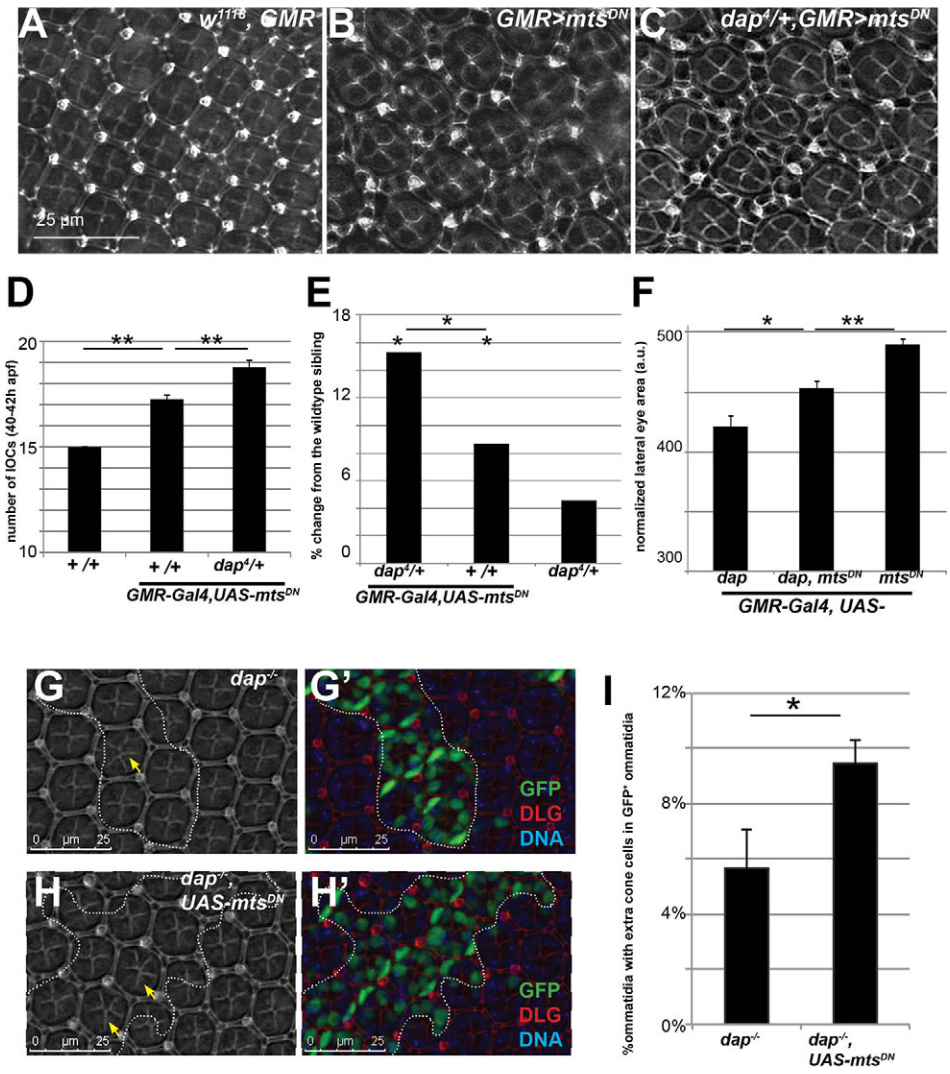

Fig. 5. PP2A genetically interacts with negative regulators of CycE/Cdk2 activity *in vivo*. (A-D) The number of IOCs is modulated by PP2A and *dap* in pupal eyes. w^{1118}, *GMR* (A) *GMR>*mts^{DN} (B), $dap^{4/+}$, *GMR>*mts^{DN} (C) pupal retinas were isolated at 42 h APF and stained for Dlg protein to determine the numbers of IOCs. IOC quantification is shown in D. Loss of one *dap* allele exacerbates the ectopic cell proliferation in pupal retinas caused by PP2A inhibition alone. (E) The lateral surface area of each adult eye was measured and compared with that of *dap+/dap+; GMR-Gal4/+* control siblings. The change in eye size is presented as the percentage change relative to the control siblings. All animals were raised under identical conditions within the same vials. Positive values represent increases in eye size. (F) The area of each adult eye for the indicated genotypes was measured in lateral view, and normalized to total head size by measurement of the distance from fronto-orbital to postvertical bristles, as animals were raised in parallel but in separate vial crosses. (G-I) GFP-labeled mutant clones were induced using the MARCM system at the early third instar larval stage. In *dap* mutant clones and in *dap* mutant clones expressing mts^{DN}, extra cone cells were quantified at 41 h APF (I). Yellow arrows indicate examples of ommatidia with extra cone cells. Error bars indicate s.e.m. n=10. *P<0.05, **P<0.01 (Student's t-test).

PP2A regulatory subunit in *Drosophila* (supplementary material Table S1) for phenotypes in the eye. We used RNAi to knockdown regulatory subunits during the final cell cycle, and compared the adult eye sizes of progeny (supplementary material Fig. S5A). Inhibition of the *Drosophila* B56 epsilon homolog (also called PPP2R5E) *widerborst* (*wdb*) led to an enlarged eye phenotype, similar to that observed with mts^{DN} expression, whereas knockdown of the B55 homolog *twins* caused a decrease in eye size, perhaps owing to defects in mitosis (Brownlee et al., 2011; Chen et al., 2007).

To test directly whether *wdb* is required for cell cycle exit, we used a dominant-negative form, wdb^{DN} (Hannus et al., 2002). Expression of wdb^{DN} driven by en^{TS}*-Gal4* during the final one to two cycles in the wing, or *GMR-Gal4* driving wdb^{RNAi} during the final cell cycle in the eye, leads to ectopic S phases and mitoses in tissues at developmental time points when they are normally quiescent (Fig. 7A; supplementary material Fig. S5C,D). We also observed ectopic E2F/DP transcriptional activity at normally postmitotic stages when *wdb* is knocked down (supplementary material Fig. S5B,I). We quantified the mitotic index in pupal tissues expressing wdb^{DN} at 26 h APF (Fig. 7C) and found that the defect in cell cycle exit upon *wdb* inhibition is less dramatic than that caused by inhibition of *mts*. We suggest that either wdb^{DN} does not completely block Wdb function or Wdb may not be the only PP2A regulatory subunit involved in the transition to quiescence and that other subunits might provide some partially overlapping functions.

Consistent with our previous tests of genetic interactions between PP2A and negative regulators of CycE/Cdk2 activity, we observed that adult eye size is increased by 15% in *dap* heterozygotes expressing wdb^{DN}, compared with dap^{WT} siblings (Fig. 7E). Inhibition of *wdb* alone causes a ~8% increase in adult eye size, suggesting that loss of one copy of *dap* synergizes with inhibition of *wdb*, similar to the genetic interaction that we observed with *mts*.

We next tested whether *wdb* contributes to the role of PP2A as a barrier to limit the bypass of cell cycle exit when CycE is dysregulated *in vivo*. We examined the morphology of the ommatidial structure in pupal retinas expressing either CycE or CycE plus wdb^{DN} as described previously for Fig. 6. The expression of wdb^{DN} and CycE together dramatically enhances the number of IOCs (Fig. 7F,G), indicative of continued cycling in the late pupal retina. By contrast, when *twins* is knocked down by RNAi in the CycE-expressing background, there is no obvious difference in IOC number compared with CycE expression alone (supplementary material Fig. S5J-L). Our data thus indicate that *wdb* contributes to the role of PP2A as a barrier to limit proliferation when CycE is dysregulated in terminally differentiating tissues.

Development (2015) 142, 3033-3045 doi:10.1242/dev.120824

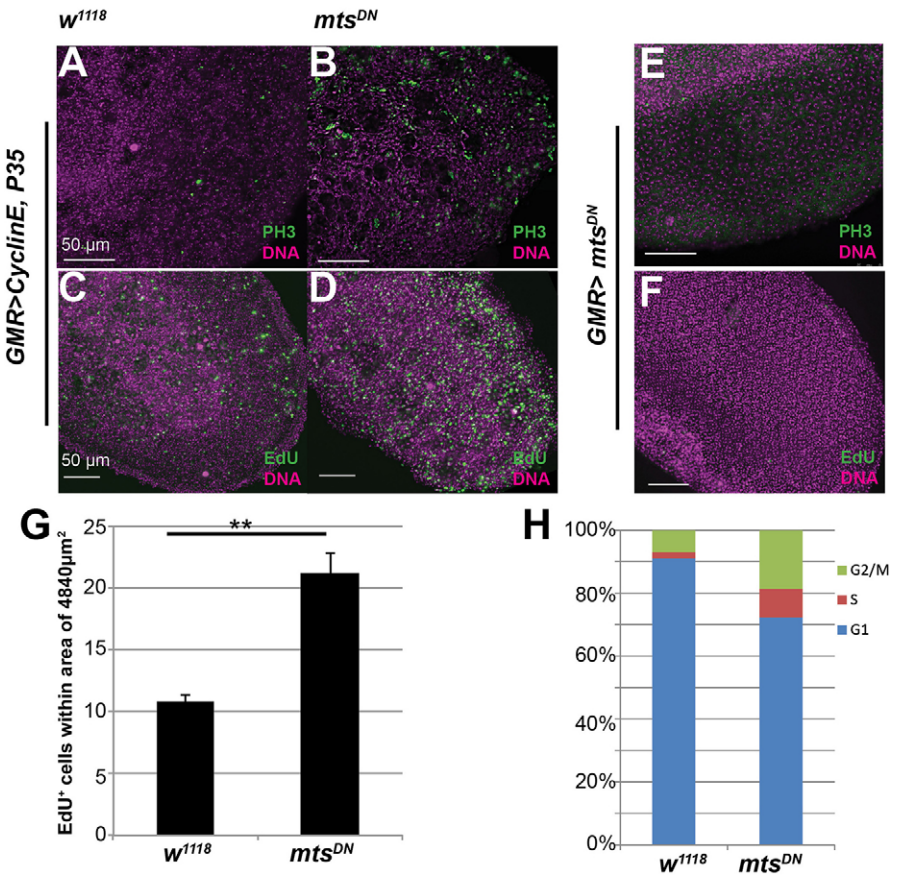

Fig. 6. Loss of PP2A function cooperates with high CycE levels to bypass cell cycle exit. (A-D) Pupal eyes expressing CycE and the apoptosis inhibitor P35 under the control of *GMR-Gal4* were stained for mitosis (with anti-PH3) or S phase (via EdU incorporation) at 40-44 h APF. Eyes with mts^{DN} expression in the presence of high CycE exhibit an increase in both EdU and PH3 staining (B,D), compared with the high CycE control (A,C). (E,F) Pupal eyes expressing mts^{DN} alone under the control of *GMR-Gal4* were stained for mitosis or S phase at 40-44 h APF. (G) EdU was quantified within a central area of the pupal eye and compared between genotypes. Error bars indicate s.e.m. n=6. $^{**}P$<0.01 (Student's t-test). (H) FACS analysis of DNA content was performed on 46 h APF pupal eyes with high CycE and mts^{DN} expression and compared with controls with high CycE. Cells with an S/G2 DNA content are increased when PP2A function is compromised.

Inhibition of PP2A increases the T-loop phosphorylation of Cdk2

Our data suggest that PP2A may promote quiescence by limiting Cdk2 activity during the final cell cycle *in vivo* to restrict proliferation in terminally differentiating tissues. To test this hypothesis, we compromised PP2A function *in vivo* by expressing mts^{DN} and CycE in the posterior larval eye under the control of the *GMR-Gal4* promoter, followed by immunoprecipitation of CycE to measure effects on CycE/Cdk2 kinase activity. When mts^{DN} is expressed in the posterior larval eye, we observe a 20-40% increase in CycE/Cdk2 kinase activity after normalization to the amount of CycE pulled down (Fig. 8A). One interpretation of this result is that PP2A knockdown leads to an increase in CycE/Cdk2 activity; however, it is also possible that the observed increase in CycE/Cdk2 kinase activity is a result of the increased proliferation that we observe when CycE is expressed under conditions in which PP2A is compromised (e.g. Fig. 6B,D) and not a direct effect of PP2A on CycE/Cdk2 activity.

To distinguish whether the increased Cdk2 activity is due to an immediate effect of PP2A inhibition on CycE/Cdk2, we performed a kinase assay in *Drosophila* S2R+ cultured cells, where we can use short-term treatments with the pan-PP2A inhibitor okadaic acid (OA) to discern immediate versus indirect effects of PP2A inhibition on CycE/Cdk2 activity. We performed a timecourse and dosage test of OA treatment in S2R+ cells and confirmed that, with 30 min of OA treatment, PP2A activity is inhibited as assessed by increased phosphorylation of S6K. We performed a timecourse of OA treatment on S2R+ cells transiently transfected with a CycE expression vector and undertook CycE/Cdk2 kinase assays as described above. We found that with 30 min of OA treatment S2R+ cells exhibit a mild increase in CycE/Cdk2 activity (Fig. 8C), consistent with a direct effect of PP2A on CycE/Cdk2 activity. However, upon longer OA treatments (2 h shown), cells exhibit a reduction in CycE/Cdk2 kinase activity and a slower migrating form of CycE protein is immunoprecipitated (Fig. 8D). In mammalian cells, PP2A/B55β can dephosphorylate the N- and C-terminal phosphodegrons of CycE1 (Tan et al., 2014). Thus, the slower migrating form of CycE that we observe might be due to inhibition of PP2A/Twins (B55) by OA in *Drosophila*, which impacts the measured CycE/Cdk2 activity.

Altogether, our data suggest that short-term inhibition of PP2A can increase CycE/Cdk2 activity, whereas prolonged loss of PP2A function impacts CycE/Cdk2 in a complex manner due to differing functions of multiple PP2A complexes. We suggest there might be a smaller contribution of PP2A/Twins complexes to the overall PP2A activity during the final cell cycle *in vivo*, as compared with actively proliferating S2R+ cells *in vitro*.

PP2A can bind and remove an activating phosphate on the T-loop of human CDK2 *in vitro* (Poon and Hunter, 1995) and the T-loop and critical activating phosphorylation sites are conserved between mammals and *Drosophila*. To test whether PP2A complexes limit CycE/Cdk2 activity after mitosis by removing the Cdk2 T-loop phosphorylation, we turned to murine cell lines in which cells can be synchronized in M phase and Cdk2 phospho-T-loop-specific antibodies are available. We synchronized NIH 3T3 mouse embryonic fibroblasts (MEFs) in M phase by nocodazole treatment to depolymerize microtubules. We then released cells from the mitotic arrest and performed a timecourse analysis of Cdk2 T-loop phosphorylation in cells treated with the pan-PP2A inhibitor OA versus vehicle only. We observed that, 8 h after release from a mitotic arrest, treatment with OA for 30 min doubles T-loop phosphorylation compared with a vehicle-treated control (Fig. 8F).

Development (2015) 142, 3033-3045 doi:10.1242/dev.120824

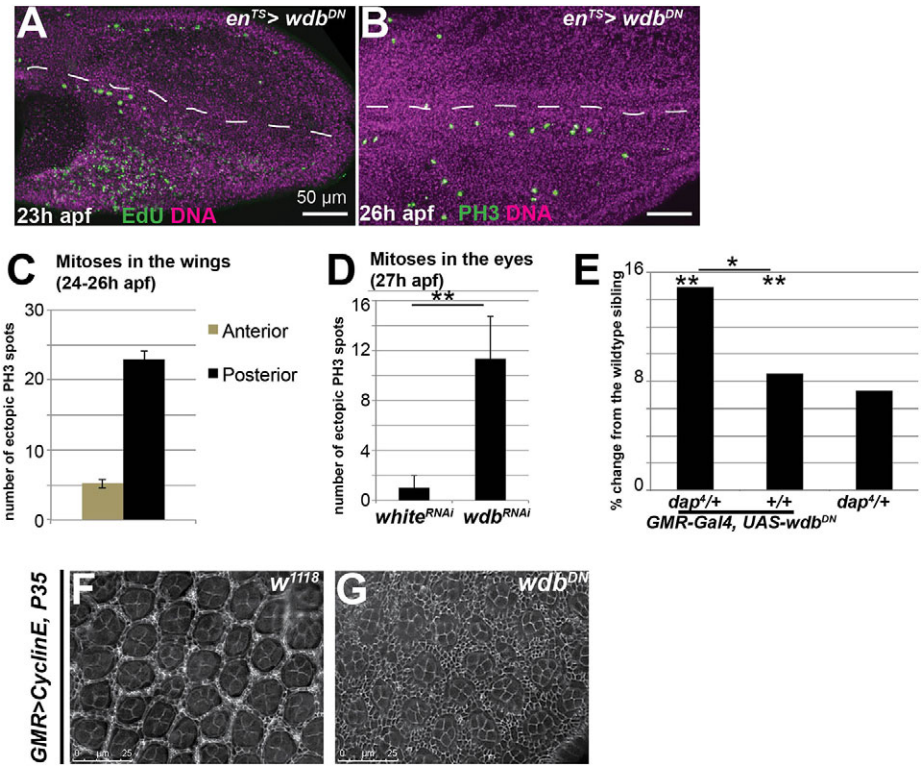

Fig. 7. The B56/Wdb regulatory subunit promotes the transition to quiescence in terminally differentiating tissues. (A,B) Dominant-negative *wdb* (*wdb*^{DN}) was expressed in the posterior wing from mid-L3 using *engrailed-Gal4/Gal80*^{TS}. Pupal tissues were labeled with EdU for 1 h at 23 h APF to visualize S phases (A) or labeled with anti-PH3 at 26 h APF to visualize mitoses (B). (C,D) Quantification of ectopic mitoses in pupal wings from 24-26 h APF (C) and eyes at 27 h APF (D). (E) Quantification of adult eye sizes shows an increase of more than 8% when *wdb*^{DN} is expressed during the final cell cycle using *GMR-Gal4*. Loss of one allele of *dap* enhances this *wdb*^{DN} phenotype, whereas loss of one allele of *dap* alone increases eye size by less than 8%. Error bars indicate s.e.m. **P*<0.05, ***P*<0.01 (Student's *t*-test). (F,G) Pupal retinas were isolated at 42 h APF and stained for Dlg to visualize IOCs in the sensitized *GMR>CycE, P35* background (F). IOC numbers increase, forming multiple layers between cone cell clusters in this background when *wdb*^{DN} is expressed (G).

We next tested whether a similar OA treatment in asynchronously proliferating MEFs could lead to an increase in Cdk2 T-loop phosphorylation. We observed a mild increase (20%) in Cdk2 T-loop phosphorylation in NIH 3T3 MEFs, whereas we detected no effect on Cdk2 T-loop phosphorylation in primary asynchronous MEFs. This suggests that redundant mechanisms may limit the effect of PP2A on the T-loop in primary cells. However, we observed a 50% increase in Cdk2 T-loop phosphorylation in *p27* (*Cdkn1b*) knockout (*p27*^{KO}) primary MEFs treated with OA (Fig. 8G), suggesting that PP2A might preferentially act on Cdk2 complexes that are not bound to Cdk inhibitors. We also observed increased levels of Cdk2 in *p27*^{KO} MEFs, suggesting the role of PP2A might be fully revealed under conditions in which CycE/Cdk2 levels are high, but need to be rapidly inhibited. This is consistent with the genetic interactions we observed in *Drosophila* between PP2A and the p27 homolog *dap*.

An interaction between *Drosophila* Wdb and Cdk2 in a yeast two-hybrid assay has been reported (Stanyon et al., 2004). To confirm whether PP2A/Wdb complexes interact with CycE/Cdk2 complexes, we performed an immunoprecipitation of endogenous CycE with a V5-tagged Wdb in proliferating S2R+ cells (supplementary material Fig. S6A). We observe a mild enrichment of CycE in samples with Wdb-V5 pulled down, compared with controls and mock precipitations. The enrichment of CycE might be mild because PP2A/Wdb interacts with many substrates in a transient manner throughout the cell cycle. We propose that only a fraction of the precipitated Wdb-V5 complexes at a given time from asynchronously proliferating cells will therefore contain endogenous CycE.

To examine this in more detail, we next transfected CycE and Wdb-V5 expression vectors into S2R+ cells, and looked for colocalization of the proteins during the cell cycle. We found that CycE and Wdb-V5 colocalize in the cytoplasm during mitosis (supplementary material Fig. S6B). CycE is predominantly nuclear, but becomes dispersed in the cytoplasm during nuclear envelope breakdown in mitosis, whereas Wdb is predominantly cytoplasmic. This suggests that PP2A/Wdb complexes most likely interact with CycE/Cdk2 complexes transiently during or just after mitosis, before nuclear envelope reformation. This is consistent with our results in NIH 3T3 cells, which suggest that the maximal effect of PP2A on the Cdk2 T-loop occurs ∼8 h after a mitotic release.

Altogether, our studies suggest that B56/PP2A can act to restrict CycE/Cdk2 activity after mitosis to promote quiescence *in vivo*.

DISCUSSION

We identify a new role for PP2A in promoting quiescence during the transition to a permanently postmitotic state in *Drosophila* wings and eyes. We observe that ∼10% of cells undergo an extra cell cycle when PP2A functions are compromised. Although this effect may appear small, the cell cycle exit mechanism *in vivo* is so robust that cells completely lacking major cell cycle regulators such as the RB family member *Rbf1* or the sole p21/p27-type CKI *dap* only exhibit a mitotic or S-phase index of 9% or less in eyes and wings (Buttitta et al., 2007; Sukhanova and Du, 2008). As with other cell cycle regulators that act redundantly to promote cell cycle exit, we see synergism when PP2A is compromised under conditions that dysregulate the G1-S Cyclin, CycE (Firth and Baker, 2005).

Cells with reduced PP2A function exhibit ectopic cell cycle markers until 13 h after normal exit timing, which is roughly consistent with the one extra cell division that we measure by clonal lineage analysis. Importantly, the ectopic proliferation phenotypes we observe are the result of manipulating PP2A functions specifically during the final one to two cell cycles, without disturbance of prior PP2A mitotic functions during active proliferation.

PP2A impacts the proliferation-quiescence decision *in vivo*

Recent studies on PP2A in the proliferation-quiescence decision have revealed that PP2A activates the RB related family member p107 by dephosphorylation to promote growth arrest in chondrocytes (Kolupaeva et al., 2008; Kurimchak et al., 2013). Another group

Development (2015) 142, 3033-3045 doi:10.1242/dev.120824

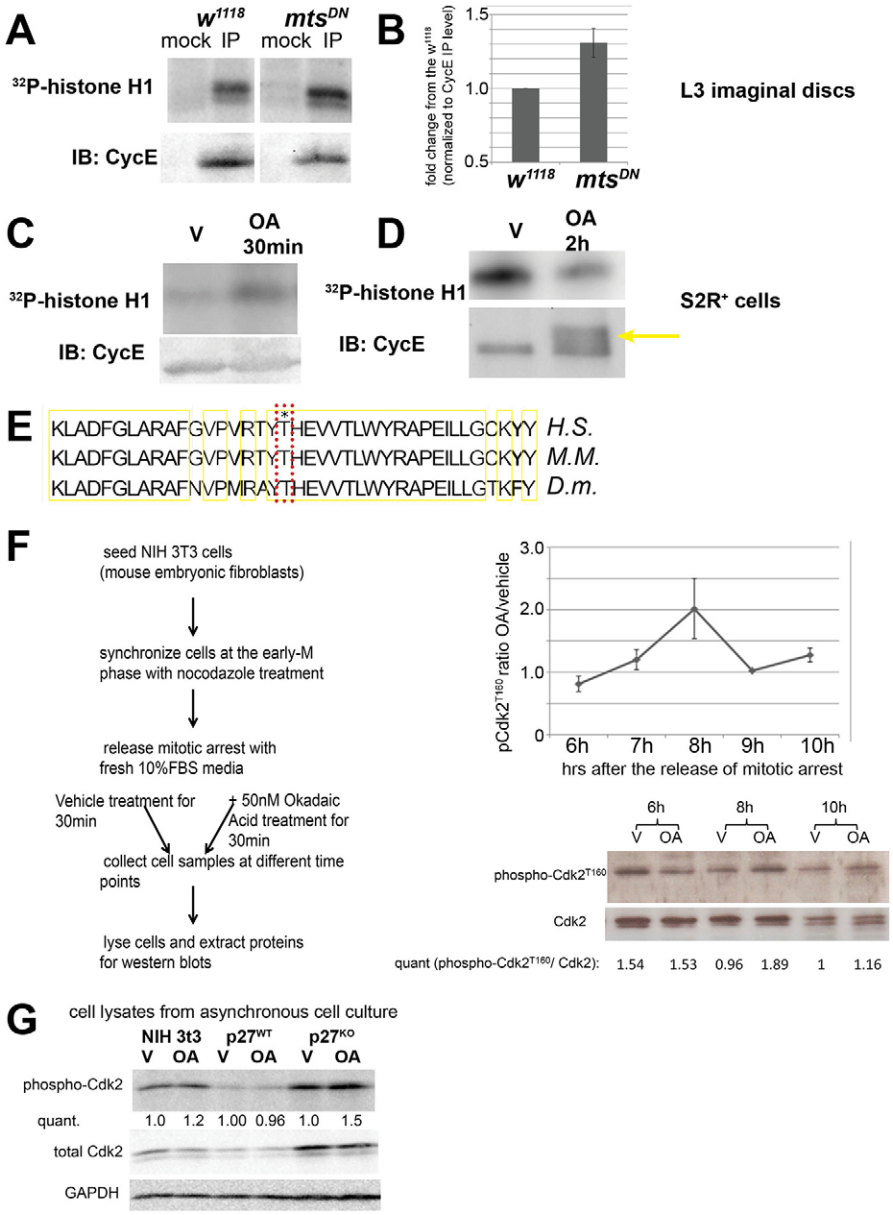

Fig. 8. PP2A affects Cdk2 T-loop phosphorylation. (A,B) CycE/Cdk2 activity was measured in an *in vitro* kinase assay using Histone H1 as a substrate. Protein samples were collected from larval eyes co-expressing CycE, the apoptosis inhibitor P35, with or without mts^{DN} under the control of *GMR-Gal4*. CycE was immunoprecipitated; mock precipitations without CycE antibody were performed with the same lysate. Error bars indicate s.e.m. (C,D) S2R+ cells transfected with a CycE expression vector were treated with 50 nM okadaic acid (OA) for 30 min or 2 h versus vehicle (DMSO) only (lanes V). Kinase assays were performed on immunoprecipitated CycE. The yellow arrow indicates a slower migrating form of CycE. (E) The T-loop phosphorylation site (asterisk, boxed) of Cdk2 is conserved in human, mouse and *Drosophila*. (F) Murine NIH 3T3 cells were arrested in G2/M using nocodazole and subsequently released from arrest. A timecourse was performed to examine endogenous Cdk2 T-loop phosphorylation in samples treated with vehicle only (V) or the PP2A inhibitor OA for 30 min at the indicated time point after nocodazole release. An outline of the experimental procedure is shown on the left. A representative blot of total Cdk2 and phospho-Cdk2 after nocodazole release is shown on the right. The line graph shows quantification of the OA-treated/vehicle-treated phospho-Cdk2 ratio with two or three independent biological replicates at each time point. Error bars indicate s.e.m. (G) In asynchronously proliferating murine NIH 3T3 cells treatment with OA causes a 20% increase in Cdk2 T-loop phosphorylation, whereas primary $p27^{WT}$ MEFs show no increase. By contrast, asynchronously proliferating $p27^{KO}$ MEFs exhibit a 50% increase in Cdk2 T-loop phosphorylation upon OA treatment.

recently found a second mechanism for PP2A to promote quiescence, whereby PP2A/B56 inhibits Ras signaling during G2 phase, which limits subsequent Myc expression and reduces CycE expression in the following G1 (Naetar et al., 2014). This promotes quiescence by limiting CycE, which would otherwise disrupt the association of RB family members with E2F/DP complexes by phosphorylation. Our data, however, suggest that there is yet another mechanism during the final cell cycle *in vivo*, independent of Ras/ERK signaling (supplementary material Fig. S7), Myc (supplementary material Fig. S7), CycE levels (supplementary material Fig. S4) and RB/E2F/DP function (Fig. 3), which promotes timely entry into quiescence. This additional mechanism acts directly on the cell cycle machinery, downstream or in parallel to RB/E2F/DP function, and appears to be crucial for the extremely robust type of developmentally controlled G0 observed *in vivo*.

B56 regulatory subunits promote quiescence *in vivo*

The emergence of multiple pathways for PP2A to promote quiescence might be a consequence of its broad functions, with impacts on various substrates in different cell cycle phases (Janssens et al., 2005; Mumby, 2007; Westermarck and Hahn, 2008; Yang and Phiel, 2010). In normal development, cells enter into the quiescent state in response to developmental signals, while in cell culture serum deprivation is most often used for synchronization in G0, via disrupted metabolic signals (Naetar et al., 2014). It might be that in these different biological contexts PP2A acts upon different targets to influence the proliferation-quiescence decision. PP2A is directed to distinct targets via the regulatory subunit, which has dynamic associations and localizations during the cell cycle. It is therefore important to note that, consistent with the recent work of Naetar et al. (2014), we also independently identified a B56 subunit (Wdb) as the main PP2A regulatory subunit promoting quiescence *in vivo*. However, our data demonstrate that *wdb* acts via a different mechanism to promote permanent cell cycle exit *in vivo*.

Most known cell cycle functions for PP2A in *Drosophila* involve the B55 regulatory subunit Twins and its roles in regulating mitotic entry and exit (Brownlee et al., 2011; Chabu and Doe, 2009; Chen et al., 2007; Wang et al., 2013, 2011). Consistent with this, when we

Development (2015) 142, 3033-3045 doi:10.1242/dev.120824

manipulate PP2A activity in early tissues, such as the actively proliferating larval wing or eye, we also observe disruptions of mitosis. An inhibitory role for PP2A in the Hippo signaling pathway, which regulates tissue growth, survival and proliferation, has also been described (Ribeiro et al., 2010). However, when PP2A inhibits Hippo signaling it acts via B‴ regulatory subunits and has exactly the opposite effect to the growth and cell cycle phenotype that we observe here. The requirement for *wdb* during the final cell cycle to promote quiescence implies that the PP2A enzyme complexes may switch from predominantly B55 (Twins) to B56 (Wdb) during the final cell cycle, mitotic exit and the subsequent G0 arrest. Understanding how the switches in PP2A regulatory subunits are regulated during the cell cycle and in response to developmental signals will be an important area for future study.

PP2A inhibits CycE/Cdk2 activity during the final cell cycle to promote quiescence

A recent study monitoring single-cell cycle dynamics in cell culture demonstrated that thresholds of Cdk2 activity after the completion of mitosis regulate the subsequent proliferation-quiescence decision (Spencer et al., 2013). Our data suggest a role for PP2A in limiting Cdk2 activity during the final cell cycle *in vivo* to restrict proliferation in terminally differentiating tissues. Inhibition of PP2A during the final cell cycle leads to ectopic Cdk2 activity, as detected via the MPM2 epitopes at the HLB (Fig. 3), and genetically cooperates with the CycE inhibitors *ago* and *dap*. In mammalian cells, PP2A inhibition after mitosis leads to an increase in the activating Cdk2 T-loop phosphorylation. It is possible that PP2A and CycE/Cdk2 also share downstream targets in cell cycle regulation, similar to the role of PP2A/B55 complexes in reversing Cdk1 phosphorylation of mitotic targets. However, we could not confirm any effect of PP2A genetic manipulations on the phosphorylation of *Drosophila* Rbf, an important target of CycE/Cdk2 activity for cell cycle exit in flies (Meyer et al., 2000) (supplementary material Fig. S6C). We suggest that PP2A/Wdb acts to modulate CycE/Cdk2 activity during the final cell cycle to help promote rapid and timely induction of G0 during development.

MATERIALS AND METHODS

Fly stocks

For a list of fly stocks, see supplementary material Table S2.

Histology and antibodies

Pupae, staged from white pre-pupae (0 h APF) at 25°C, were dissected and fixed as described (Buttitta et al., 2007). Pupal cuticle was removed from wings post fixation. Note that the wing hinge and notum were excluded from our quantifications. Hoechst 33258 (Molecular Probes, 1 µg/ml) was used to label nuclei. Antibodies used: rabbit anti-phospho-Histone H3 (Ser10) (Upstate, #06-570; 1:4000), mouse anti-MPM2 (Upstate, #05-368; 1:200), rabbit anti-GFP (Molecular Probes, A11122; 1:1000), mouse anti-CycB (DSHB, F2F4; 1:100), mouse anti-Discs large (DSHB, 4F3; 1:100) and anti-*Drosophila* Dp (gift from Dr M. Frolov; Frolov et al., 2005). Appropriate secondary antibodies were Alexa 488, 568 or 633 conjugated (Molecular Probes) or HRP conjugated (Jackson ImmunoResearch) and used at 1:4000. 5-ethynyl-2′-deoxyuridine (EdU) incorporation was performed using the Click-iT EdU Alexa Fluor 555 Imaging Kit (Life Technologies).

IOC counting

IOCs are shared by adjacent ommatidial cores, and the number of IOCs is quantified within an ommatidial group (OG) that covers a defined hexagonal area (bordered by the yellow dots in Fig. 2) with its apices being the adjacent ommatidial centers. Those secondary pigment cells crossed by the dashed lines were counted as half. At least 15 OGs were scored from independent samples for each genotype, following the method of Ou et al. (2007).

Clonal analysis

Clones were induced by heat shock for 7 min at 37°C between 48 and 70 h after egg deposition in a *hsflp; tub>CD2>Gal4, UAS-GFP; tub-Gal80^{TS}, UAS-Diap* background. Animals were aged at 18°C (permissive for Gal80^{TS}, Gal4 OFF), and shifted to 28°C (non-permissive for Gal80^{TS}, Gal4 ON) at late L3 instar larval stage, collected at 0 h APF and aged to different stages in metamorphosis. Experiments using *engrailed*-Gal4 with Gal80^{TS} were carried out in the same way, except that experiments restricting transgene expression to the final cell cycle were shifted to 28°C at 0 h APF. By phenotypic analyses and GFP visualization, we confirmed complete inhibition of Gal4 in the lines used here with Gal80^{TS} at 18°C, and we detected activation of target genes within 6 h of shifting to 29°C. Development at 28°C proceeds 1.15 times faster than at 25°C, and at 45% of the 25°C rate at 18°C (Ashburner, 1989). All incubation times were adjusted accordingly. Hours APF are presented as the equivalent time at 25°C for simplicity. Loss-of-function clones were generated using MARCM (Lee and Luo, 2001). Larvae were heat shocked for 20 min at 37°C at early third larval instar, collected for staging at 0 h APF, aged at 25°C and dissected at the times indicated.

Clonal cell counts to quantify cell divisions

Non-overlapping clones labeled with GFP and expressing the indicated transgenes were induced at 0 h APF (white prepupae) with 2 min heat shock at 37°C. Wings were dissected and fixed 40-42 h later, nuclei were labeled with 1 µg/ml Hoechst 33258, and GFP-positive cells per clone were scored blind on a Leica DMI6000 microscope. Cells per clone were counted blind for at least 100 clones in the wing blade and the average cell number per clone reflects the number of cell divisions undergone before exit. We excluded clones in the wing margin, hinge, notum area and hemocytes in the veins. Transgenic expression of an apoptosis inhibitor (UAS-P35) was used in the clonal cell count experiments, including all controls.

Flow cytometry

Dissociation of cells from staged, dissected pupae and FACS were carried out as previously described (Flegel et al., 2013). All experiments were carried out at least three times; representative examples are shown.

Western blotting and kinase assays

Antibodies used: rabbit anti-CycE (Santa Cruz, sc-33748; 1:1000), goat anti-CycE (Santa Cruz, sc-15905; 1:200), mouse anti-CycA (DSHB, A12; 1:1000), mouse anti-CycB (DSHB; 1:1000), rabbit anti-phospho-Cdc2 (Cell Signaling, #9111; 1:1000), rabbit anti-Cdc2 (Upstate, #06-923; 1:1000), anti-phospho-S6K (Thr398) (Cell Signaling, #9209; 1:333), anti-*Drosophila* Myc (Santa Cruz, sc-28207; 1:1000), anti-dpERK (Sigma, M8159; 1:500), anti-pERK (Cell Signaling, #4370; 1:1000), anti-HA probe (Santa Cruz, sc-805; 1:1000), anti-mouse phospho-Cdk2^{T160} (Cell Signaling, #2561; 1:500), anti-mouse Cdk2 (Santa Cruz, M2, sc-163; 1:1000), anti-*Drosophila* Rbf (DX3; Lee et al., 2012), anti-α-tubulin (DSHB, 12G10; 1:1000), anti-β-tubulin (DSHB, E7; 1:1000), anti-γ-tubulin (Sigma, T6557; 1:1000) and anti-mouse GAPDH (Cell Signaling, 14C10; 1:2000) were used as loading controls with the appropriate HRP-conjugated secondary antibody. Enhanced chemiluminescence (ECL) detection (Amersham) followed by digital imaging (to prevent signal saturation, Bio-Rad) was performed and band signal intensity was quantified using ImageJ (NIH).

For kinase assays, cell lysates were collected either from late L3 imaginal discs or S2R+ cells transfected with pMT-Cyclin E. For the S2R+ cells, 30 min or 2 h OA (50 nM) treatment was performed before cell harvest. For further details, see Guest et al. (2011).

Microscopy

Images were obtained using a Zeiss LSM 510 confocal or Leica DMI6000 epifluorescence system with deconvolution (ImageQuant). All images were

cropped, rotated and processed using Adobe Photoshop. For brightness/contrast the Auto Contrast function was used. All brightness/contrast adjustments were applied equally on the entire image. Adult eye images were obtained using a Leica MZ10F microscope and a Nikon Ds-Vi1 digital camera. All adult eye images were measured using Nikon NIS Elements D software and processed with Adobe Photoshop.

Cell culture

D. melanogaster S2R+ cells were cultured at 25°C in Schneider's Insect Medium supplemented with 10% fetal bovine serum (FBS). NIH 3T3, $p27^{WT}$ and $p27^{KO}$ MEFs were cultured at 37°C, 5% CO_2 in Dulbecco's Modified Eagle Medium (DMEM) supplemented with 10% FBS. For cell cycle synchronization, NIH 3T3 cells were treated with 200 ng/µl nocodazole for 18-20 h. The constructs pMT-Wdb-V5 and pMT-Cyclin E were transiently transfected using FuGENE (Roche) and expressed by copper induction (0.5 mM) in S2R+ cells.

Acknowledgements

We thank Drs M. Frolov, H. Richardson, S. Eaton, Y. Chabu, H. Wang, Y. Su, R. Duronio and the Bloomington Stock Center [NIH P40OD018537] for flies; Drs J. E. Lee, C. Y. Lee, C. Duan and the Developmental Studies Hybridoma Bank for antibodies; Drs R. Smith-Bolton, K. Cadigan and C. Y. Lee for helpful comments on the manuscript; Dr B. Edgar, in whose lab the initial pilot RNAi screen for cell cycle exit regulators was performed; Dr J. Nandakumar and lab members for their help and advice on kinase and pulldown assays; Dr A. Minella for providing $p27^{WT}$ and $p27^{KO}$ MEFs; and Sapha Hassan and Kerry Flegel for technical assistance.

Competing interests

The authors declare no competing or financial interests.

Author contributions

D.S. and L.B. developed the approach, performed the experiments and prepared the manuscript.

Funding

This work was supported by a National Institutes of Health grant [R00GM086517 to L.B.], the Biological Sciences Scholars Program (BSSP) and startup funding from the University of Michigan. Deposited in PMC for release after 12 months.

Supplementary material

Supplementary material available online at
http://dev.biologists.org/lookup/suppl/doi:10.1242/dev.120824/-/DC1

References

Ashburner, M. (1989). *Drosophila: A Laboratory Handbook*. Cold Spring Harbor, NY: Cold Spring Harbor Laboratory Press.

Bandura, J. L., Jiang, H., Nickerson, D. W. and Edgar, B. A. (2013). The molecular chaperone Hsp90 is required for cell cycle exit in Drosophila melanogaster. *PLoS Genet.* **9**, e1003835.

Baumgardt, M., Karlsson, D., Salmani, B. Y., Bivik, C., MacDonald, R. B., Gunnar, E. and Thor, S. (2014). Global programmed switch in neural daughter cell proliferation mode triggered by a temporal gene cascade. *Dev. Cell* **30**, 192-208.

Bielinski, V. A. and Mumby, M. C. (2007). Functional analysis of the PP2A subfamily of protein phosphatases in regulating Drosophila S6 kinase. *Exp. Cell Res.* **313**, 3117-3126.

Binné, U. K., Classon, M. K., Dick, F. A., Wei, W., Rape, M., Kaelin, W. G., Jr, Näär, A. M. and Dyson, N. J. (2007). Retinoblastoma protein and anaphase-promoting complex physically interact and functionally cooperate during cell-cycle exit. *Nat. Cell Biol.* **9**, 225-232.

Brownlee, C. W., Klebba, J. E., Buster, D. W. and Rogers, G. C. (2011). The protein phosphatase 2A regulatory subunit Twins stabilizes Plk4 to induce centriole amplification. *J. Cell Biol.* **195**, 231-243.

Buck, S. B., Bradford, J., Gee, K. R., Agnew, B. J., Clarke, S. T. and Salic, A. (2008). Detection of S-phase cell cycle progression using 5-ethynyl-2′-deoxyuridine incorporation with click chemistry, an alternative to using 5-bromo-2′-deoxyuridine antibodies. *Biotechniques* **44**, 927-929.

Buttitta, L. A., Katzaroff, A. J., Perez, C. L., de la Cruz, A. and Edgar, B. A. (2007). A double-assurance mechanism controls cell cycle exit upon terminal differentiation in Drosophila. *Dev. Cell* **12**, 631-643.

Buttitta, L. A., Katzaroff, A. J. and Edgar, B. A. (2010). A robust cell cycle control mechanism limits E2F-induced proliferation of terminally differentiated cells in vivo. *J. Cell Biol.* **189**, 981-996.

Chabu, C. and Doe, C. Q. (2009). Twins/PP2A regulates aPKC to control neuroblast cell polarity and self-renewal. *Dev. Biol.* **330**, 399-405.

Chen, P. and Segil, N. (1999). p27(Kip1) links cell proliferation to morphogenesis in the developing organ of Corti. *Development* **126**, 1581-1590.

Chen, F., Archambault, V., Kar, A., Lio', P., D'Avino, P. P., Sinka, R., Lilley, K., Laue, E. D., Deak, P., Capalbo, L. et al. (2007). Multiple protein phosphatases are required for mitosis in Drosophila. *Curr. Biol.* **17**, 293-303.

Coller, H. A. (2011). Cell biology. The essence of quiescence. *Science* **334**, 1074-1075.

Datar, S. A., Jacobs, H. W., de la Cruz, A. F., Lehner, C. F. and Edgar, B. A. (2000). The Drosophila cyclin D-Cdk4 complex promotes cellular growth. *EMBO J.* **19**, 4543-4554.

de Nooij, J. C., Letendre, M. A. and Hariharan, I. K. (1996). A cyclin-dependent kinase inhibitor, Dacapo, is necessary for timely exit from the cell cycle during Drosophila embryogenesis. *Cell* **87**, 1237-1247.

Ehmer, U., Zmoos, A.-F., Auerbach, R. K., Vaka, D., Butte, A. J., Kay, M. A. and Sage, J. (2014). Organ size control is dominant over Rb family inactivation to restrict proliferation in vivo. *Cell Rep.* **8**, 371-381.

Ellis, M. C., O'Neill, E. M. and Rubin, G. M. (1993). Expression of Drosophila glass protein and evidence for negative regulation of its activity in non-neuronal cells by another DNA-binding protein. *Development* **119**, 855-865.

Evans, D. R. H., Myles, T., Hofsteenge, J. and Hemmings, B. A. (1999). Functional expression of human PP2Ac in yeast permits the identification of novel C-terminal and dominant-negative mutant forms. *J. Biol. Chem.* **274**, 24038-24046.

Fero, M. L., Rivkin, M., Tasch, M., Porter, P., Carow, C. E., Firpo, E., Polyak, K., Tsai, L.-H., Broudy, V., Perlmutter, R. M. et al. (1996). A syndrome of multiorgan hyperplasia with features of gigantism, tumorigenesis, and female sterility in p27Kip1-deficient mice. *Cell* **85**, 733-744.

Firth, L. C. and Baker, N. E. (2005). Extracellular signals responsible for spatially regulated proliferation in the differentiating Drosophila eye. *Dev. Cell* **8**, 541-551.

Flegel, K., Sun, D., Grushko, O., Ma, Y. and Buttitta, L. (2013). Live cell cycle analysis of Drosophila tissues using the attune acoustic focusing cytometer and Vybrant DyeCycle violet DNA stain. *J. Vis. Exp.*, e50239.

Frolov, M. V., Moon, N.-S. and Dyson, N. J. (2005). dDP is needed for normal cell proliferation. *Mol. Cell. Biol.* **25**, 3027-3039.

Grosskortenhaus, R. and Sprenger, F. (2002). Rca1 inhibits APC-Cdh1Fzr and is required to prevent cyclin degradation in G2. *Dev. Cell* **2**, 29-40.

Guest, S. T., Yu, J., Liu, D., Hines, J. A., Kashat, M. A. and Finley, R. L., Jr. (2011). A protein network-guided screen for cell cycle regulators in Drosophila. *BMC Syst. Biol.* **5**, 65.

Gui, H., Li, S. and Matise, M. P. (2007). A cell-autonomous requirement for Cip/Kip cyclin-kinase inhibitors in regulating neuronal cell cycle exit but not differentiation in the developing spinal cord. *Dev. Biol.* **301**, 14-26.

Hahn, K., Miranda, M., Francis, V. A., Vendrell, J., Zorzano, A. and Teleman, A. A. (2010). PP2A regulatory subunit PP2A-B′ counteracts S6K phosphorylation. *Cell Metab.* **11**, 438-444.

Hannus, M., Feiguin, F., Heisenberg, C. P. and Eaton, S. (2002). Planar cell polarization requires Widerborst, a B' regulatory subunit of protein phosphatase 2A. *Development* **129**, 3493-3503.

Hunt, T. (2013). On the regulation of protein phosphatase 2A and its role in controlling entry into and exit from mitosis. *Adv. Biol. Regul.* **53**, 173-178.

Jacobs, H. W., Keidel, E. and Lehner, C. F. (2001). A complex degradation signal in Cyclin A required for G1 arrest, and a C-terminal region for mitosis. *EMBO J.* **20**, 2376-2386.

Janssens, V., Goris, J. and Van Hoof, C. (2005). PP2A: the expected tumor suppressor. *Curr. Opin. Genet. Dev.* **15**, 34-41.

Jayadeva, G., Kurimchak, A., Garriga, J., Sotillo, E., Davis, A. J., Haines, D. S., Mumby, M. and Grana, X. (2010). B55alpha PP2A holoenzymes modulate the phosphorylation status of the retinoblastoma-related protein p107 and its activation. *J. Biol. Chem.* **285**, 29863-29873.

Kiyokawa, H., Kineman, R. D., Manova-Todorova, K. O., Soares, V. C., Hoffman, E. S., Ono, M., Khanam, D., Hayday, A. C., Frohman, L. A. and Koff, A. (1996). Enhanced growth of mice lacking the cyclin-dependent kinase inhibitor function of p27Kip1. *Cell* **85**, 721-732.

Kolupaeva, V. and Janssens, V. (2013). PP1 and PP2A phosphatases - cooperating partners in modulating retinoblastoma protein activation. *FEBS J.* **280**, 627-643.

Kolupaeva, V., Laplantine, E. and Basilico, C. (2008). PP2A-mediated dephosphorylation of p107 plays a critical role in chondrocyte cell cycle arrest by FGF. *PLoS ONE* **3**, e3447.

Kurimchak, A. and Grana, X. (2013). PP2A counterbalances phosphorylation of pRB and mitotic proteins by multiple CDKs: potential implications for PP2A disruption in cancer. *Genes Cancer* **3**, 739-748.

Kurimchak, A., Haines, D. S., Garriga, J., Wu, S., De Luca, F., Sweredoski, M. J., Deshaies, R. J., Hess, S. and Grana, X. (2013). Activation of p107 by fibroblast growth factor, which is essential for chondrocyte cell cycle exit, is mediated by the protein phosphatase 2A/B55alpha holoenzyme. *Mol. Cell. Biol.* **33**, 3330-3342.

Lane, M. E., Sauer, K., Wallace, K., Jan, Y. N., Lehner, C. F. and Vaessin, H. (1996). Dacapo, a cyclin-dependent kinase inhibitor, stops cell proliferation during Drosophila development. *Cell* **87**, 1225-1235.
Lee, T. and Luo, L. (2001). Mosaic analysis with a repressible cell marker (MARCM) for Drosophila neural development. *Trends Neurosci.* **24**, 251-254.
Lee, H., Ragusano, L., Martinez, A., Gill, J. and Dimova, D. K. (2012). A dual role for the dREAM/MMB complex in the regulation of differentiation-specific E2F/RB target genes. *Mol. Cell. Biol.* **32**, 2110-2120.
Loeb, K. R., Kostner, H., Firpo, E., Norwood, T., Tsuchiya, K. D., Clurman, B. E. and Roberts, J. M. (2005). A mouse model for cyclin E-dependent genetic instability and tumorigenesis. *Cancer Cell* **8**, 35-47.
Lohmann, I., McGinnis, N., Bodmer, M. and McGinnis, W. (2002). The Drosophila Hox gene deformed sculpts head morphology via direct regulation of the apoptosis activator reaper. *Cell* **110**, 457-466.
Meyer, C. A., Jacobs, H. W., Datar, S. A., Du, W., Edgar, B. A. and Lehner, C. F. (2000). Drosophila Cdk4 is required for normal growth and is dispensable for cell cycle progression. *EMBO J.* **19**, 4533-4542.
Milan, M., Campuzano, S. and Garcia-Bellido, A. (1996). Cell cycling and patterned cell proliferation in the Drosophila wing during metamorphosis. *Proc. Natl. Acad. Sci. USA* **93**, 11687-11692.
Minella, A. C., Loeb, K. R., Knecht, A., Welcker, M., Varnum-Finney, B. J., Bernstein, I. D., Roberts, J. M. and Clurman, B. E. (2008). Cyclin E phosphorylation regulates cell proliferation in hematopoietic and epithelial lineages in vivo. *Genes Dev.* **22**, 1677-1689.
Moberg, K. H., Bell, D. W., Wahrer, D. C., Haber, D. A. and Hariharan, I. K. (2001). Archipelago regulates Cyclin E levels in Drosophila and is mutated in human cancer cell lines. *Nature* **413**, 311-316.
Mumby, M. (2007). PP2A: unveiling a reluctant tumor suppressor. *Cell* **130**, 21-24.
Naetar, N., Soundarapandian, V., Litovchick, L., Goguen, K. L., Sablina, A. A., Bowman-Colin, C., Sicinski, P., Hahn, W. C., DeCaprio, J. A. and Livingston, D. M. (2014). PP2A-mediated regulation of Ras signaling in G2 is essential for stable quiescence and normal G1 length. *Mol. Cell* **54**, 932-945.
Nakayama, K., Ishida, N., Shirane, M., Inomata, A., Inoue, T., Shishido, N., Horii, I., Loh, D. Y. and Nakayama, K.,-i. (1996). Mice lacking p27Kip1 display increased body size, multiple organ hyperplasia, retinal dysplasia, and pituitary tumors. *Cell* **85**, 707-720.
Neufeld, T. P., de la Cruz, A. F. A., Johnston, L. A. and Edgar, B. A. (1998). Coordination of growth and cell division in the Drosophila wing. *Cell* **93**, 1183-1193.
Nicolay, B. N. and Frolov, M. V. (2008). Context-dependent requirement for dE2F during oncogenic proliferation. *PLoS Genet.* **4**, e1000205.
Nicolay, B. N., Bayarmagnai, B., Moon, N. S., Benevolenskaya, E. V. and Frolov, M. V. (2010). Combined inactivation of pRB and hippo pathways induces dedifferentiation in the Drosophila retina. *PLoS Genet.* **6**, e1000918.
Ou, C.-Y., Wang, C.-H., Jiang, J. and Chien, C.-T. (2007). Suppression of Hedgehog signaling by Cul3 ligases in proliferation control of retinal precursors. *Dev. Biol.* **308**, 106-119.
Pajcini, K. V., Corbel, S. Y., Sage, J., Pomerantz, J. H. and Blau, H. M. (2010). Transient inactivation of Rb and ARF yields regenerative cells from postmitotic mammalian muscle. *Cell Stem Cell* **7**, 198-213.
Pignoni, F. and Zipursky, S. L. (1997). Induction of Drosophila eye development by decapentaplegic. *Development* **124**, 271-278.
Poon, R. Y. C. and Hunter, T. (1995). Dephosphorylation of Cdk2 Thr160 by the cyclin-dependent kinase-interacting phosphatase KAP in the absence of cyclin. *Science* **270**, 90-93.
Ribeiro, P. S., Josué, F., Wepf, A., Wehr, M. C., Rinner, O., Kelly, G., Tapon, N. and Gstaiger, M. (2010). Combined functional genomic and proteomic approaches identify a PP2A complex as a negative regulator of Hippo signaling. *Mol. Cell* **39**, 521-534.
Ruggiero, R., Kale, A., Thomas, B. and Baker, N. E. (2012). Mitosis in neurons: Roughex and APC/C maintain cell cycle exit to prevent cytokinetic and axonal defects in Drosophila photoreceptor neurons. *PLoS Genet.* **8**, e1003049.
Saucedo, L. J., Gao, X., Chiarelli, D. A., Li, L., Pan, D. and Edgar, B. A. (2003). Rheb promotes cell growth as a component of the insulin/TOR signalling network. *Nat. Cell Biol.* **5**, 566-571.
Schubiger, M. and Palka, J. (1987). Changing spatial patterns of DNA replication in the developing wing of Drosophila. *Dev. Biol.* **123**, 145-153.
Simon, F., Fichelson, P., Gho, M. and Audibert, A. (2009). Notch and Prospero repress proliferation following cyclin E overexpression in the Drosophila bristle lineage. *PLoS Genet.* **5**, e1000594.
Spencer, S. L., Cappell, S. D., Tsai, F.-C., Overton, K. W., Wang, C. L. and Meyer, T. (2013). The proliferation-quiescence decision is controlled by a bifurcation in CDK2 activity at mitotic exit. *Cell* **155**, 369-383.
Stanyon, C. A., Liu, G., Mangiola, B. A., Patel, N., Giot, L., Kuang, B., Zhang, H., Zhong, J. and Finley, R. L., Jr. (2004). A Drosophila protein-interaction map centered on cell-cycle regulators. *Genome Biol.* **5**, R96.
Sukhanova, M. J. and Du, W. (2008). Control of cell cycle entry and exiting from the second mitotic wave in the Drosophila developing eye. *BMC Dev. Biol.* **8**, 7.
Tan, Y., Sun, D., Jiang, W., Klotz-Noack, K., Vashisht, A. A., Wohlschlegel, J., Widschwendter, M. and Spruck, C. (2014). PP2A-B55beta antagonizes cyclin E1 proteolysis and promotes its dysregulation in cancer. *Cancer Res.* **74**, 2006-2014.
Tanaka-Matakatsu, M., Thomas, B. J. and Du, W. (2007). Mutation of the Apc1 homologue shattered disrupts normal eye development by disrupting G1 cell cycle arrest and progression through mitosis. *Dev. Biol.* **309**, 222-235.
Tane, S., Ikenishi, A., Okayama, H., Iwamoto, N., Nakayama, K. I. and Takeuchi, T. (2014). CDK inhibitors, p21Cip1 and p27Kip1, participate in cell cycle exit of mammalian cardiomyocytes. *Biochem. Biophys. Res. Commun.* **443**, 1105-1109.
Thacker, S. A., Bonnette, P. C. and Duronio, R. J. (2003). The contribution of E2F-regulated transcription to Drosophila PCNA gene function. *Curr. Biol.* **13**, 53-58.
Tomlinson, A. and Ready, D. F. (1987). Cell fate in the Drosophila ommatidium. *Dev. Biol.* **123**, 264-275.
Wang, C., Chang, K. C., Somers, G., Virshup, D., Ang, B. T., Tang, C., Yu, F. and Wang, H. (2009). Protein phosphatase 2A regulates self-renewal of Drosophila neural stem cells. *Development* **136**, 3031-3031.
Wang, P., Pinson, X. and Archambault, V. (2011). PP2A-twins is antagonized by greatwall and collaborates with polo for cell cycle progression and centrosome attachment to nuclei in drosophila embryos. *PLoS Genet.* **7**, e1002227.
Wang, P., Galan, J. A., Normandin, K., Bonneil, E., Hickson, G. R., Roux, P. P., Thibault, P. and Archambault, V. (2013). Cell cycle regulation of Greatwall kinase nuclear localization facilitates mitotic progression. *J. Cell Biol.* **202**, 277-293.
Westermarck, J. and Hahn, W. C. (2008). Multiple pathways regulated by the tumor suppressor PP2A in transformation. *Trends Mol. Med.* **14**, 152-160.
White, A. E., Leslie, M. E., Calvi, B. R., Marzluff, W. F. and Duronio, R. J. (2007). Developmental and cell cycle regulation of the Drosophila histone locus body. *Mol. Biol. Cell* **18**, 2491-2502.
White, A. E., Burch, B. D., Yang, X.-c., Gasdaska, P. Y., Dominski, Z., Marzluff, W. F. and Duronio, R. J. (2011). Drosophila histone locus bodies form by hierarchical recruitment of components. *J. Cell Biol.* **193**, 677-694.
Wirt, S. E., Adler, A. S., Gebala, V., Weimann, J. M., Schaffer, B. E., Saddic, L. A., Viatour, P., Vogel, H., Chang, H. Y., Meissner, A. et al. (2010). G1 arrest and differentiation can occur independently of Rb family function. *J. Cell Biol.* **191**, 809-825.
Wu, J. Q., Hansen, D. V., Guo, Y., Wang, M. Z., Tang, W., Freel, C. D., Tung, J. J., Jackson, P. K. and Kornbluth, S. (2007). Control of Emi2 activity and stability through Mos-mediated recruitment of PP2A. *Proc. Natl. Acad. Sci. USA* **104**, 16564-16569.
Yang, J. and Phiel, C. (2010). Functions of B56-containing PP2As in major developmental and cancer signaling pathways. *Life Sci.* **87**, 659-666.
Zindy, F., Cunningham, J. J., Sherr, C. J., Jogal, S., Smeyne, R. J. and Roussel, M. F. (1999). Postnatal neuronal proliferation in mice lacking Ink4d and Kip1 inhibitors of cyclin-dependent kinases. *Proc. Natl. Acad. Sci. USA* **96**, 13462-13467.

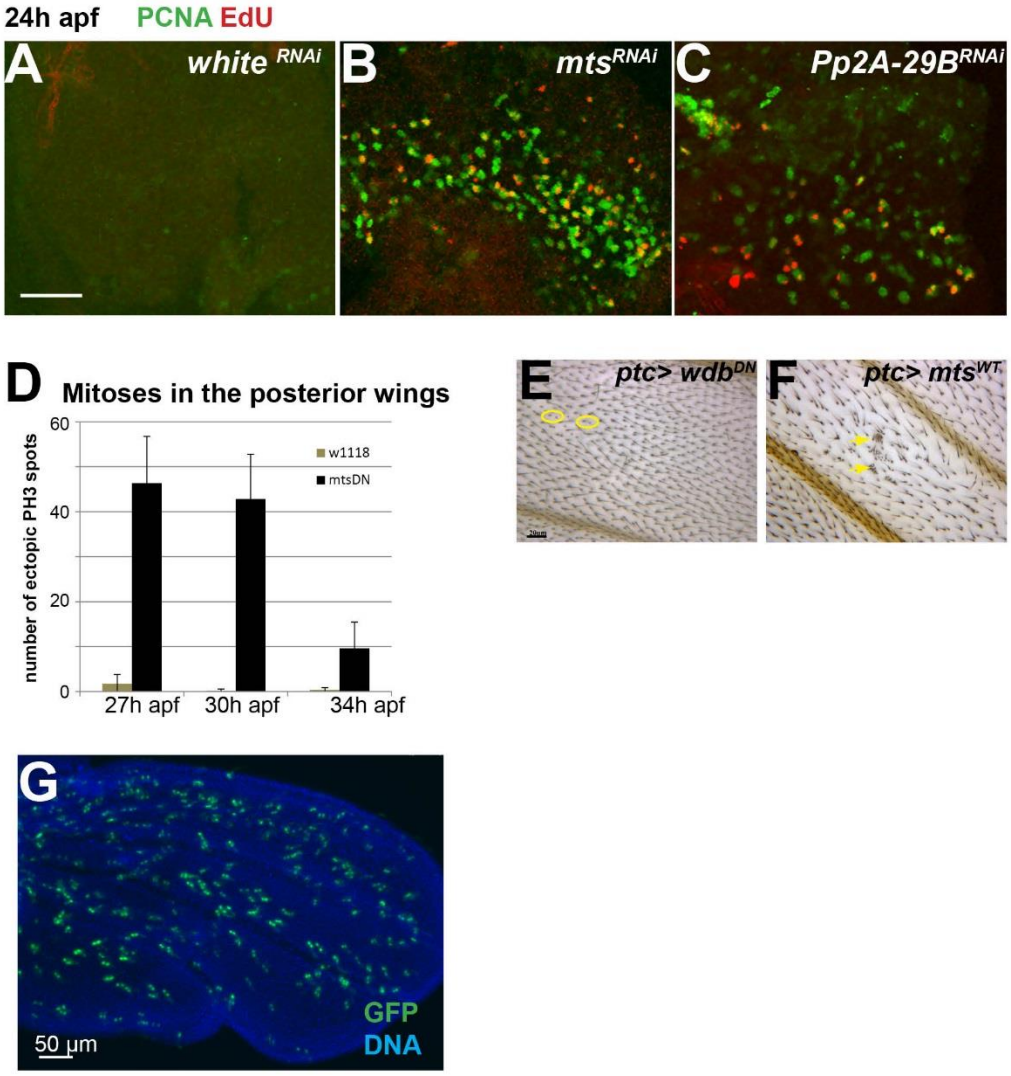

Fig. S1. Loss of PP2A activity delays the transition to quiescence *in vivo*. (A-C) The catalytic subunit (*mts*) or the scaffold subunit (*Pp2A-29B*) of PP2A was knocked down with RNAi transgenes expressed in the eye during the final cell cycle using *GMR-Gal4/UAS* and compared to a control (*white*) RNAi. Pupal tissues were isolated at 24h APF and labeled with EdU for 1 h to visualize S-phase. Expression of a PCNA-GFP reporter was used as a readout of ectopic E2F/DP transcriptional activity in eyes. Contrast and gain were increased in the control sample to show there is no reporter activity or EdU incorporation. (D) bar graph shows counts of mitoses posterior to posterior in pupal wings at developmental stages (E,F)

The indicated transgenes were expressed along the anterior-posterior boundary of the wing under the control of *patched-Gal4/UAS* and adult wings were examined for wing hair phenotypes. Note that wdb^{DN} causes a loss of wing hair (yellow circles), whereas overexpression of *mts* leads to a multiple wing hairs phenotype (arrows), consistent with (Hannus et al., 2002). Supplemental Table 1 shows the components of PP2A complexes in mammals and in *Drosophila*. (G) A representative image from the clonal lineage tracing experiment in Fig. 2A. GFP-labeled clones with mts^{DN} expression were induced at 0h APF, and pupal wings were dissected at 42- 44h APF.

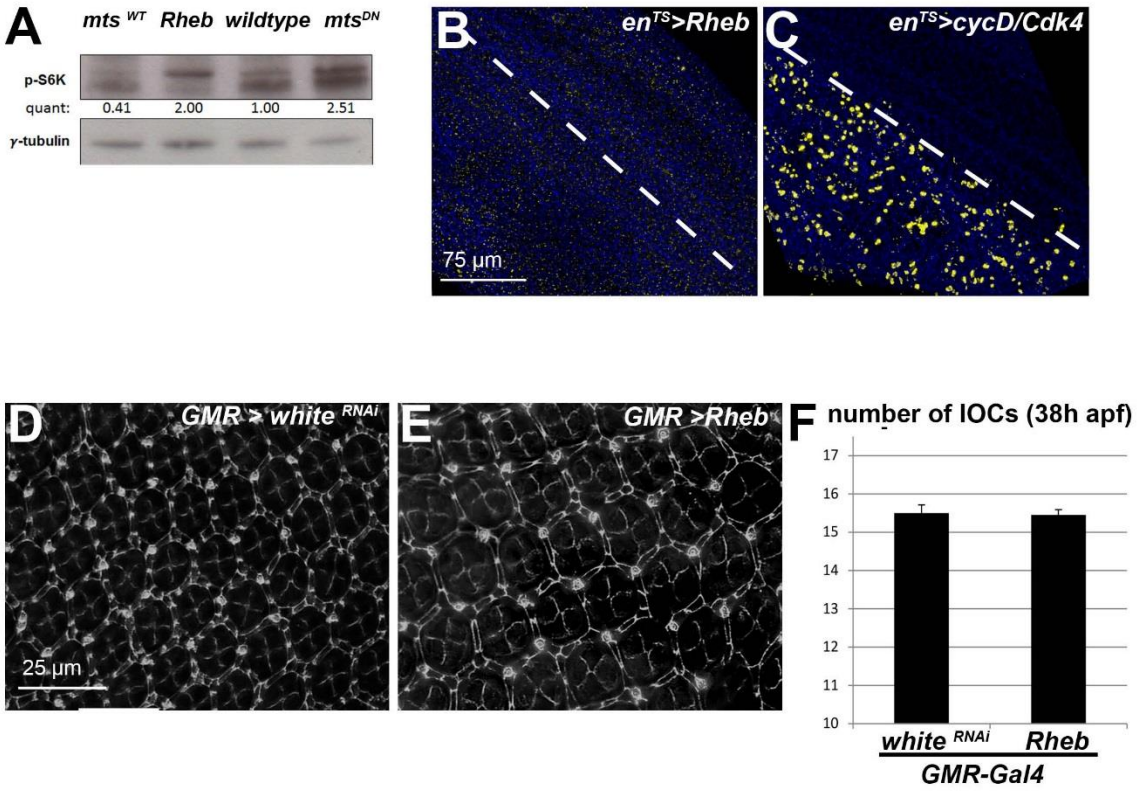

Fig. S2. Activation of the TOR/S6K pathway does not delay the transition to quiescence. (A)The indicated transgenes were induced by the *hsflp actin>Gal4/UAS* system, with a 30min heat-shock to drive expression throughout the animal. Protein was extracted from larval heads and phospho-S6K levels were determined by western blots. (B-C) The indicated transgenes were expressed in the posterior compartment of pupal wings from 0h APF using *en-Gal4/Gal80^{TS}*. Tissues were collected at 26h APF and labeled with anti-PH3 to visualize mitoses. No mitoses were observed in the posterior wing when *Rheb* (an activator of TOR) is overexpressed. By contrast, overexpression of *CyclinD/Cdk4* serves as a positive control to demonstrate delayed quiescence. (D-F) Assessment of interommatidial cell (IOC) number in 38h APF eyes in which *GMR-Gal4* drives expression of *white* RNAi (D) or *Rheb* (E). Pupal retinas were stained for Dlg, and the numbers of IOCs were quantified in panel F (N=10). IOC number is not increased in eyes expressing Rheb compared to a control RNAi.

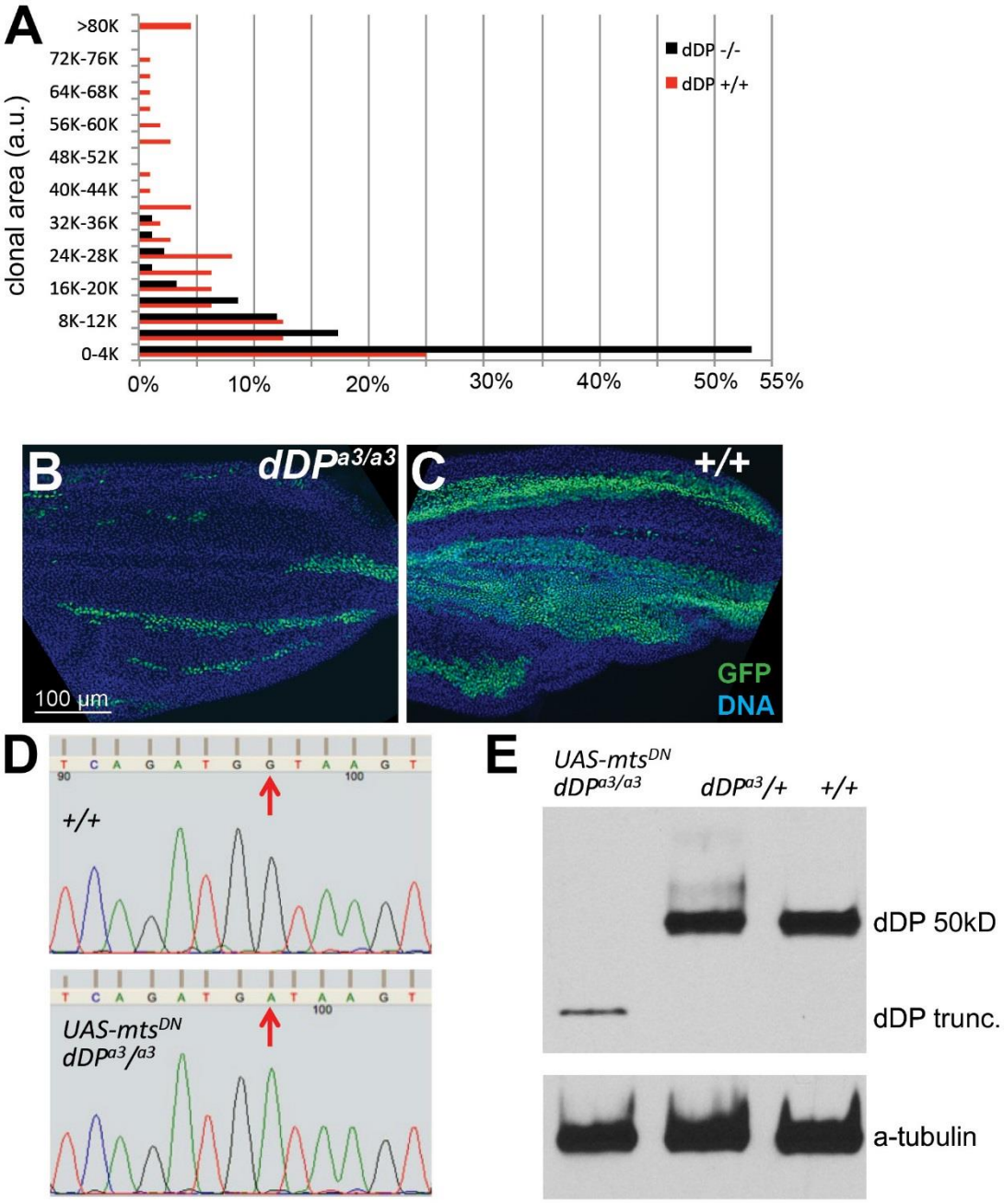

Fig. S3 *Dp* null mutant clones have a proliferation defect.

Wild type or Dp^{a3} null mutant clones were induced using the MARCM system by a 20 min heat shock at 37°C at early L3 instar larval stage. Clones were examined and measured at 24-26h APF. (A) The majority of dDp^{a3} null mutant clones (~95%) are below 20,000 (arbitrary unit) in size, while almost 40% of wild type clones were above 20,000 in size. (B,C) Wild

type ordDp^{a3} null mutant clones were induced in parallel and are marked by GFP expression. (D) Sequencing of the $dDp^{a3/a3}$,*UAS-mts*^{DN} fly line confirmes the expected point mutation in previously reported in the Dp^{a3} allele (Frolov et al., 2005). (E) Western blots for Dp expression were performed on samples extracted from wild type, heterozygous or homozygous dDp^{a3},*UAS-mts*^{DN} animals. $Dp^{a3/a3}$,*UAS-mts*^{DN} homozygotes express only a truncated form of Dp as previously reported (Frolov et al., 2005).

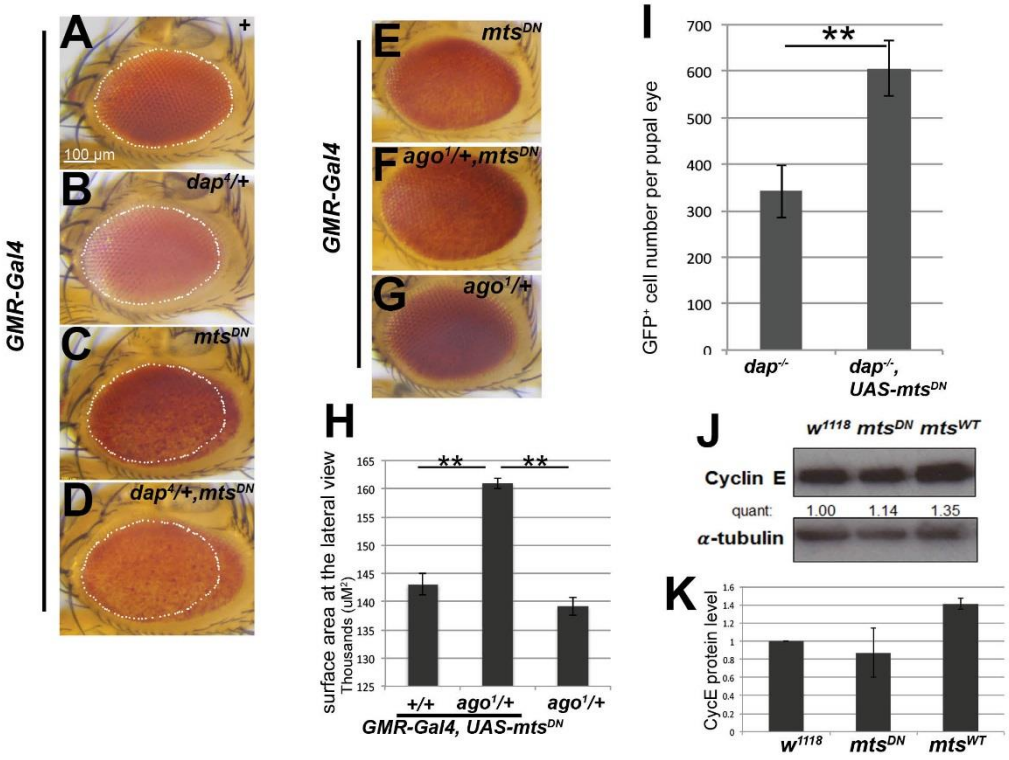

Fig. S4. PP2A genetically interacts with negative regulators of Cyclin E/Cdk2 activity *in vivo*. (A-D) Representative adult eye images used for quantifications in Fig. 5E. The white dots outline the control eye size for comparison. *GMR-Gal4*-mediated mts^{DN} expression causes a large eye phenotype (C) which is enhanced by the loss of one copy of *dap* (D). (E-H) Loss of one copy of *ago* enhances the mts^{DN} large eye phenotype. P-values were determined by Student's *t*-tests (**, P< 0.01). (E-G) Adult eye examples used for quantification in Fig. S5H. (I) GFP labeled dap^4 clones were induced using MARCM at early third instar larval stage. *dap* mutant clones and *dap* mutant clones expressing mts^{DN} were induced in parallel and examined at 41h APF. The total number of GFP positive cells per eye was compared between genotypes. (J-K) Western blots were performed to measure Cyclin E protein levels upon manipulation of PP2A activity. Protein samples were extracted from late third instar imaginal discs with the indicated transgenes expressed via *GMR-Gal4/UAS*. Quantification of signal intensities from western blots of two independent experimental replicates are shown (K).

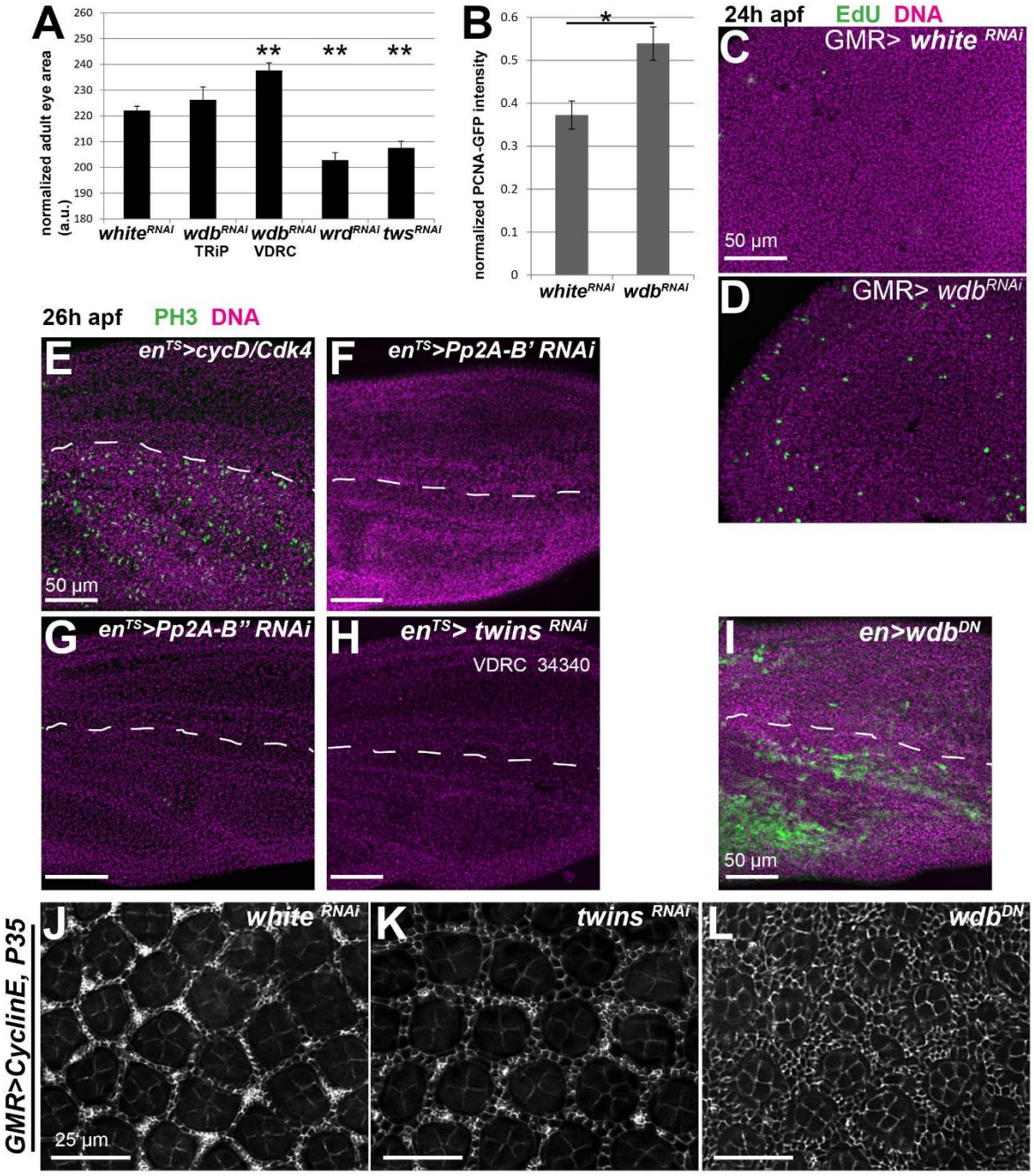

Fig. S5. The B56/*wdb* regulatory subunit promotes the transition to quiescence in terminally differentiating tissues. Flies were raised at 31°C with *GMR-Gal4/UAS* expression of the indicated RNAi transgenes to regulatory subunits of PP2A. (A) Quantification of adult female fly eye size was normalized to total body size. Asterisks indicate *p*-values determined by a Student's *t* test (**p*<0.05 ***p*<0.01). (B) Quantification of

PCNA-GFP expression in *GMR-Gal4/UAS* control (*white* RNAi) or *wdb RNAi* expressing pupal eyes at 24h APF. (C,D) Pupal eyes expressing the indicated transgenes driven by *GMR-Gal4/UAS* were labeled for 1 hour at 24h APF with EdU to visualize S phases. (E-H) Pupal wings expressing the indicated transgenes driven by *en-Gal4/Gal80^{TS}* at 26h APF were labeled with anti-PH3 to visualize mitoses (I) 24h APF pupal wings expressing *wdb^{DN}* in the posterior region driven by *en-gal4/UAS* display ectopic PCNA-GFP reporter activity. (J-L) Anti-Dlg staining was used to assess pupal eye morphology at 42-44h APF in a sensitized background with *GMR-Gal4/UAS* driving Cyclin E and P35 expression as well as the indicated transgenes.

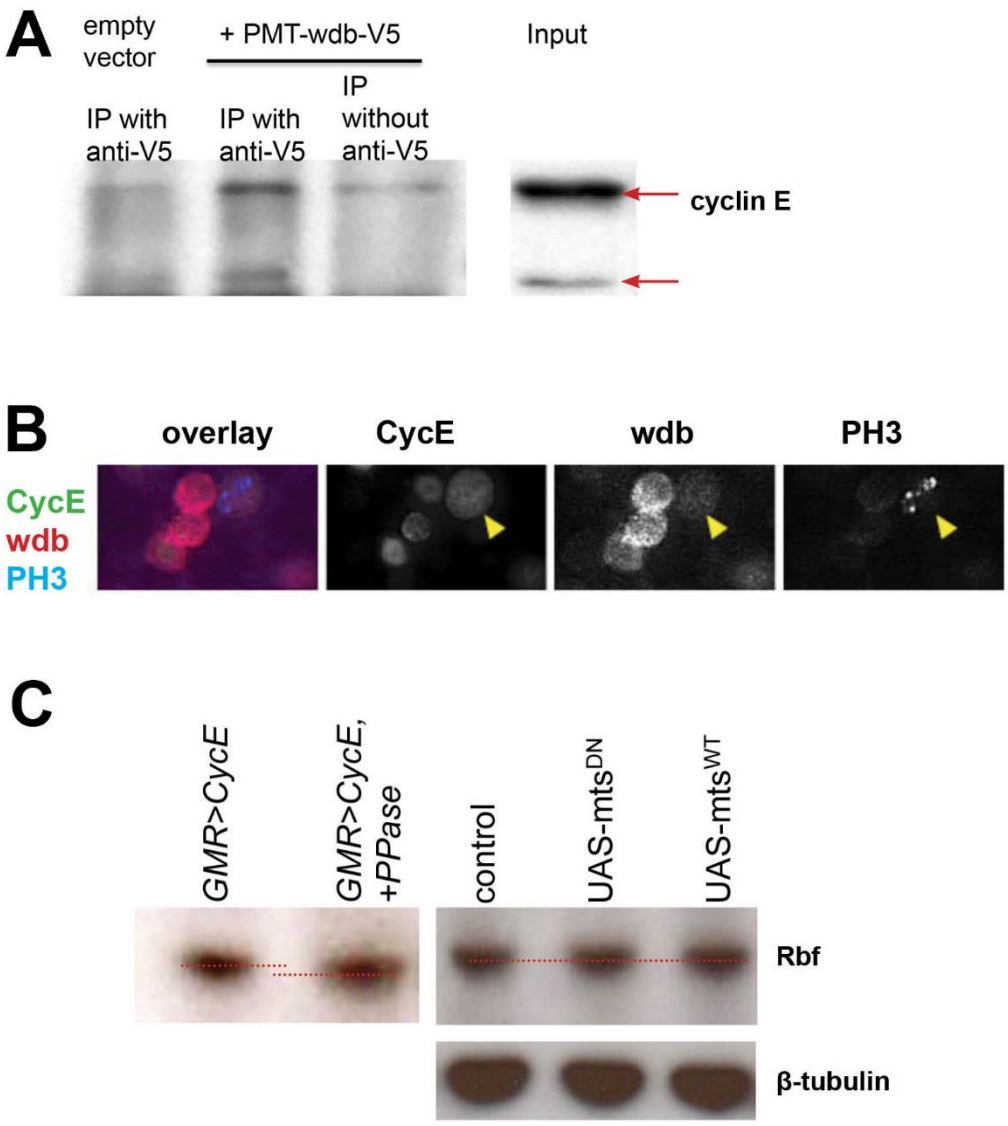

Fig. S6. Wdb interacts with Cyclin E. (A) Lysates were prepared from S2R+ cells transfected with a pMT-Wdb-V5 expression plasmid, and an anti-V5 (or mock) pulldown was performed. Enrichment of endogenous Cyclin E was observed in the V5-pulldown. Note that in S2R+ cells two different size Cyclin E protein products are expressed (66 and 77 kDa). (B) S2R+ cells were transfected with a pMT-Wdb-V5 expression plasmid and a pMT-Cyclin E expression plasmid, and fixed and stained with anti-V5 to detect Wdb, anti-Cyclin E and anti-PH3 to detect cells in mitosis. The arrow indicates a cell in mitosis where Cyclin E becomes localized to the cytoplasm. (C) Lysates were collected from late third instar larval

heads with PP2A transgene expression induced by the *hs*-Flp *actin*>Gal4/UAS system or from late third instar larval eyes expressing CycE and the apoptosis inhibitor P35 under control of *GMR-Gal4*. Lysates were resolved on a NuPAGE Bis/Tris Gel as described (Lee et al., 2012) and blotted with anti-Rbf antibody (DX3). Lysate from larvae expressing Cyclin E was split, and one half was treated with lambda phosphatase (New England Biolabs) while the other half was not, to visualize the altered migration of phosphorylated Rbf. The phosphatase treated sample shows a subtle shift in migration, while no alteration of Rbf migration is observed in samples with genetic manipulations either increasing or inhibiting PP2A activity.

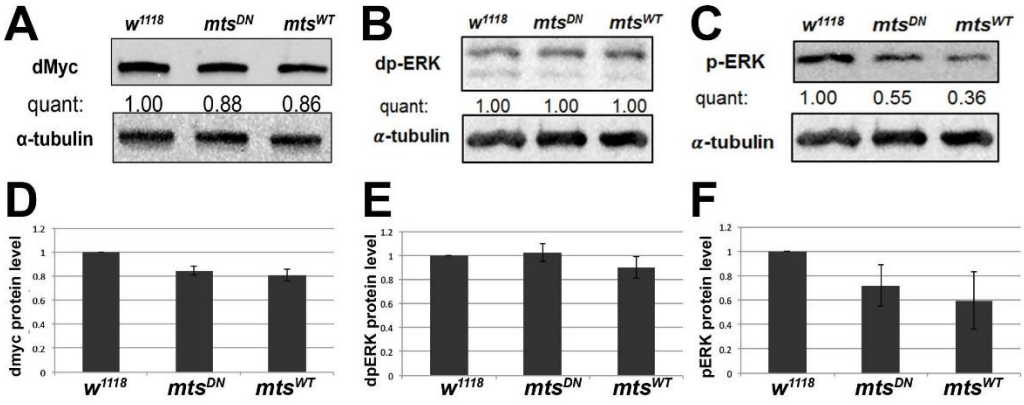

Fig. S7. Inhibition of PP2A during the final cell cycle does not increase signaling through ERK, levels of dMyc. (A-C) Western blots were performed to measure Myc and phospho-ERK (p-ERK) protein levels upon manipulation of PP2A activity. Protein samples were extracted from late third instar larval eye imaginal discs with the indicated transgenes expressed via *GMR-Gal4/UAS* to manipulate PP2A activity specifically during the final cell cycle. Note that compromising PP2A activity does not up-regulate mono p-ERK or diphospho (dp) –ERK, nor alter the migration of Myc protein. Quantifications of protein signal intensity on western blots were shown in (D-F), which represents two independent experiments.

Table S1. The components of PP2A complex

Subunits	**Description**	**Mammals**	***Drosophila***
C	catalytic subunit	PP2A-Cα, PP2A-Cβ	**mts**
A	scaffolding subunit	PP2A-Aα(PR65α), PP2A-Aβ(PR65β)	**Pp2A-29B**
B	regulatory subunit	B55α B55β B55γ B55δ	**twins/tws/aar**
B’	regulatory subunit	B56α B56β B56ε B56γ_1 γ_2 γ_3 B56δ	**PP2A-B’/wrd/B56-1**
			widerborst/wdb
			CG32568(sequence similarity)
B’’	regulatory subunit	PR72, PR48, PR130,PR59	**PP2A-B’’/CG4733/dPR72**
B’’’	regulatory subunit	striatin (PR110), SG2NA	**Cka**

Table S2. Fly stocks

Stock	Reference or source
w^{1118}	BL 5905
y w hsflp^{122};+;UAS-CycE,UAS-Cdk2	Buttitta et al., 2007
y w hsflp^{122};UAS-CycD,UAS-Cdk4;+	Datar et al., 2000
y w hsflp^{122};UAS-CycA;+	Jacobs et al., 2001
y w hsflp^{122}; UAS-Stg/CyO-GFP; +	Neufeld et al., 1998
y w hsflp^{122};+;UAS-Dacapo	Neufeld et al., 1998
y w hsflp^{122}; +; UAS-HA-Rca1/TM6B	(Zielke, Querings, Grosskortenhaus, Reis, & Sprenger, 2006)
y w hsflp^{122};+;UAS-Rbf	Neufeld et al., 1998
y w hsflp^{122};+;UAS-Rbf ^{RNAi}	VDRC 10696
w;tub>CD2>gal4,UAS-GFP;tub-gal80^{TS},UAS-Diap	UAS-Diap from Lohmann et al., 2002
w;UAS-P35;act>CD2>gal4,UAS-GFP$_{NLS}$	Neufeld et al., 1998
FRT42D,Dp^{a3}/CyO-GFP;+	Frolov et al., 2005
w;FRT42D,dap^{4}/CyO-GFP	Lane et al., 1996
w;FRT82B ago^{1}/TM6B	Moberg et al., 2001
y w hsflp^{122},tub-gal4,UAS-GFP;FRT42D tub-gal80	(Jiang et al., 2009)
y w hsflp^{122};GMR-gal4;PCNA-GFP	Bandura et al., 2013

w; GMR-gal4, UAS-CycE; GMR-P35	Kindly provided by H. Richardson, Peter MacCallum Cancer Center, Australia
w; GMR-gal4; Dr/TM6B	(T. Wang, Lao, & Edgar, 2009)
w; en-gal4,UAS-GFP; tub-gal80^{TS}	(Buttitta & Edgar, 2007)
UAS-P35;+;sb/TM6B	Neufeld et al., 1998
UAS-mts^{DN}	Chabu and Doe, 2009
UAS-mts^{WT}	Wang et al., 2009
UAS-wdb^{DN}	Hannus et al., 2002

References:

Jiang, H., Patel, P. H., Kohlmaier, A., Grenley, M. O., McEwen, D. G., & Edgar, B. A. (2009). Cytokine/Jak/Stat signaling mediates regeneration and homeostasis in the Drosophila midgut. *Cell*, *137*(7), 1343–55. doi:10.1016/j.cell.2009.05.014

Wang, C., Chang, K. C., Somers, G., Virshup, D., Ang, B. T., Tang, C., … Wang, H. (2009). Protein phosphatase 2A regulates self-renewal of Drosophila neural stem cells. *Development*, *136*(17), 3031–3031. doi:10.1242/dev.042432

Wang, T., Lao, U., & Edgar, B. A. (2009). TOR-mediated autophagy regulates cell death in Drosophila neurodegenerative disease. *The Journal of Cell Biology*, *186*(5), 703–11. doi:10.1083/jcb.200904090

Zielke, N., Querings, S., Grosskortenhaus, R., Reis, T., & Sprenger, F. (2006). Molecular dissection of the APC/C inhibitor Rca1 shows a novel F-box-dependent function. *EMBO Reports*, *7*(12), 1266–72. doi:10.1038/sj.embor.7400851